THE TEXAS GRENVILLE OROGEN, LLANO UPLIFT, TEXAS

Fieldtrip guide to the Precambrian Geology of the Llano Uplift, central Texas

by

Sharon Mosher, Mark Helper, and Jamie Levine

Department of Geological Sciences, Jackson School of Geosciences, University of Texas at Austin

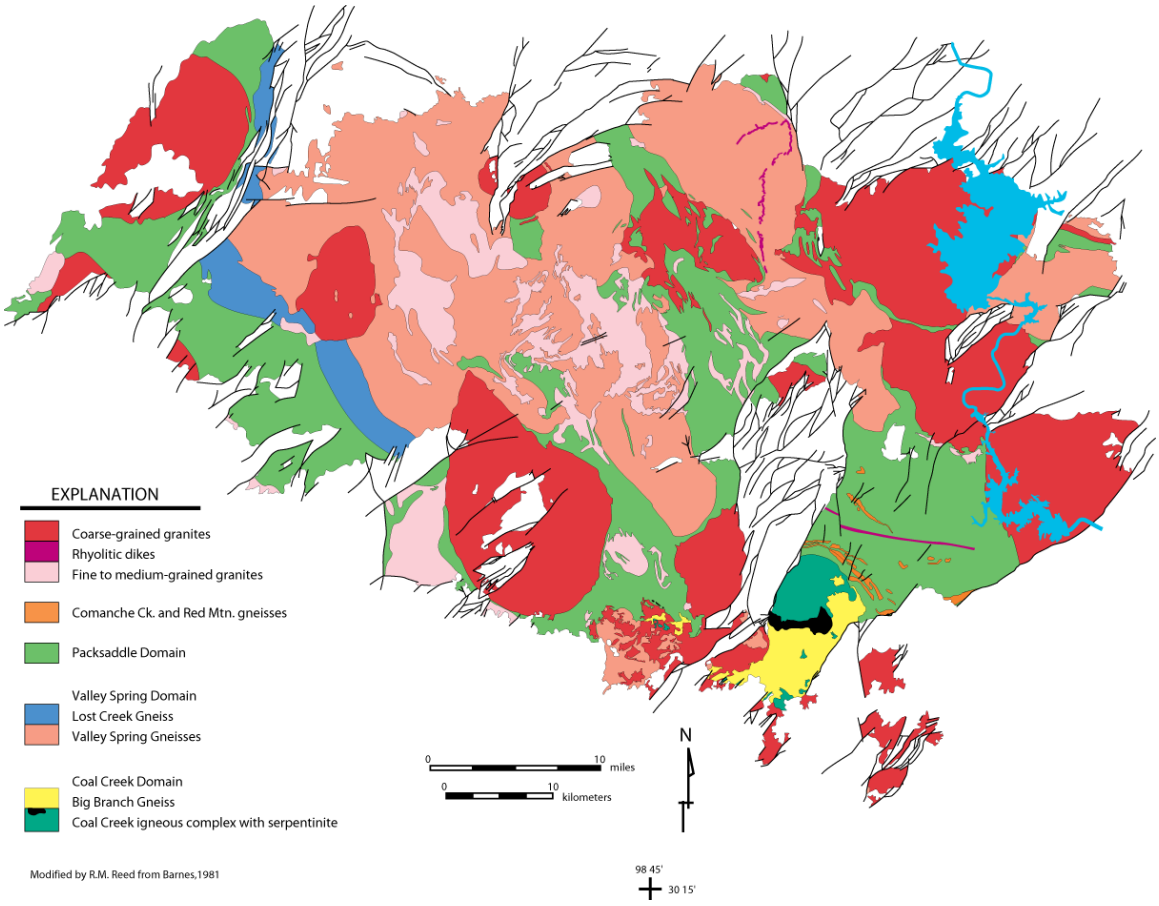

TRIP 405 for THE GEOLOGICAL SOCIETY OF AMERICA ANNUAL MEETING, HOUSTON, TX, FALL 2008

Cosponsored by GSA Structural Geology and Tectonics Division

THE TEXAS GRENVILLE OROGEN, LLANO UPLIFT, TEXAS

Fieldtrip guide to the Precambrian Geology of the Llano Uplift, central Texas

by

Sharon Mosher, Mark Helper, and Jamie Levine

Department of Geological Sciences, Jackson School of Geosciences, University of Texas at Austin

TRIP 405 for THE GEOLOGICAL SOCIETY OF AMERICA ANNUAL MEETING, HOUSTON, TX, FALL 2008

Cosponsored by GSA Structural Geology and Tectonics Division

Cover:
Robert M. Reed

GEOLOGY OF THE LLANO UPLIFT

by Sharon Mosher

INTRODUCTION

The Llano Uplift of central Texas consists of multiply deformed, 1.37-1.23 Ga metasedimentary, metavolcanic and metaplutonic rocks intruded by 1.13 to 1.07 Ga, syn-tectonic to post-tectonic granites (Fig. 1) (Mosher, 1998). An early high-pressure eclogite-facies metamorphism is overprinted by dynamothermal, medium-pressure metamorphism at upper amphibolite-facies conditions and a subsequent low-pressure, middle amphibolite-facies metamorphism associated with widespread intrusion of late granites (Carlson et al., 2007). These rocks are exposed in a gentle structural dome exposing ~9000 km^2 of Middle Proterozoic crystalline basement in an erosional window through Phanerozoic sedimentary cover (Muehlberger et al., 1967; Flawn and Muehlberger, 1970). Normal and oblique-slip faults related to the Ouachita Orogeny affect Precambrian to Pennsylvanian rocks and juxtapose Paleozoic strata with the Precambrian exposures. The entire uplift is unconformably overlain by the Cretaceous.

On this field trip, we will make a transect across the eastern uplift on Day 1 looking at three distinct lithologic/structural domains and the polyphase deformation and metamorphism with them. We will begin in the south with the Coal Creek domain, a lesser deformed tonalitic to dioritic island arc terrane, and move northwards through the Packsaddle domain, a polydeformed, highly transposed supracrustal sequence of metaplutonic, metavolcanic and metasedimentary rocks, and then into the Valley Spring domain, a polydeformed granitic gneiss terrane with relict eclogitic bodies. On Day 2 we visit Valley Spring and Packsaddle outcrops in the western uplift to compare lithologic, structural, metamorphic and age relationships with those in the eastern uplift. We will examine the late stage granites that intrude all domains. (Stops on both days are shown on Figure 2.)

Lithotectonic Domains

Coal Creek Domain. The Coal Creek domain consists of a 1326 Ma-1275 Ma tonalitic to dioritic plutonic complex and ophiolitic rocks, interpreted to represent part of an exotic island arc terrane and obducted oceanic crust (Garrison, 1985; Roback, 1996). The Coal Creek domain shows an intrusive, deformational, and metamorphic history unique to that of the rest of the uplift (Roback et al., 1994: Roback, 1996). A large tabular body of serpentinized harzburgite in the interior of the domain is in tectonic contact with the igneous rocks and shows a complex history of serpentinization, metamorphism, and deformation (Gillis, 1989). Other associated ophiolitic material includes Fe-rich low to medium K_2O metabasalts and cumulate metagabbros with chemistry similar to island arc and abyssal tholeiites, hornblendites, and mafic schists (Garrison, 1982). South of the serpentinite is a fairly monotonous, 1326-1301 Ma, folded, well-foliated, gray, mafic to tonalitic gneiss (Big Branch Gneiss). North of the serpentinite, this gneiss crops out locally and is cross cut by a younger, cogenetic dioritic to tonalitic suite (Coal Creek igneous complex) (Roback, 1996) (Fig. 3). Primary, cross cutting intrusive relationships

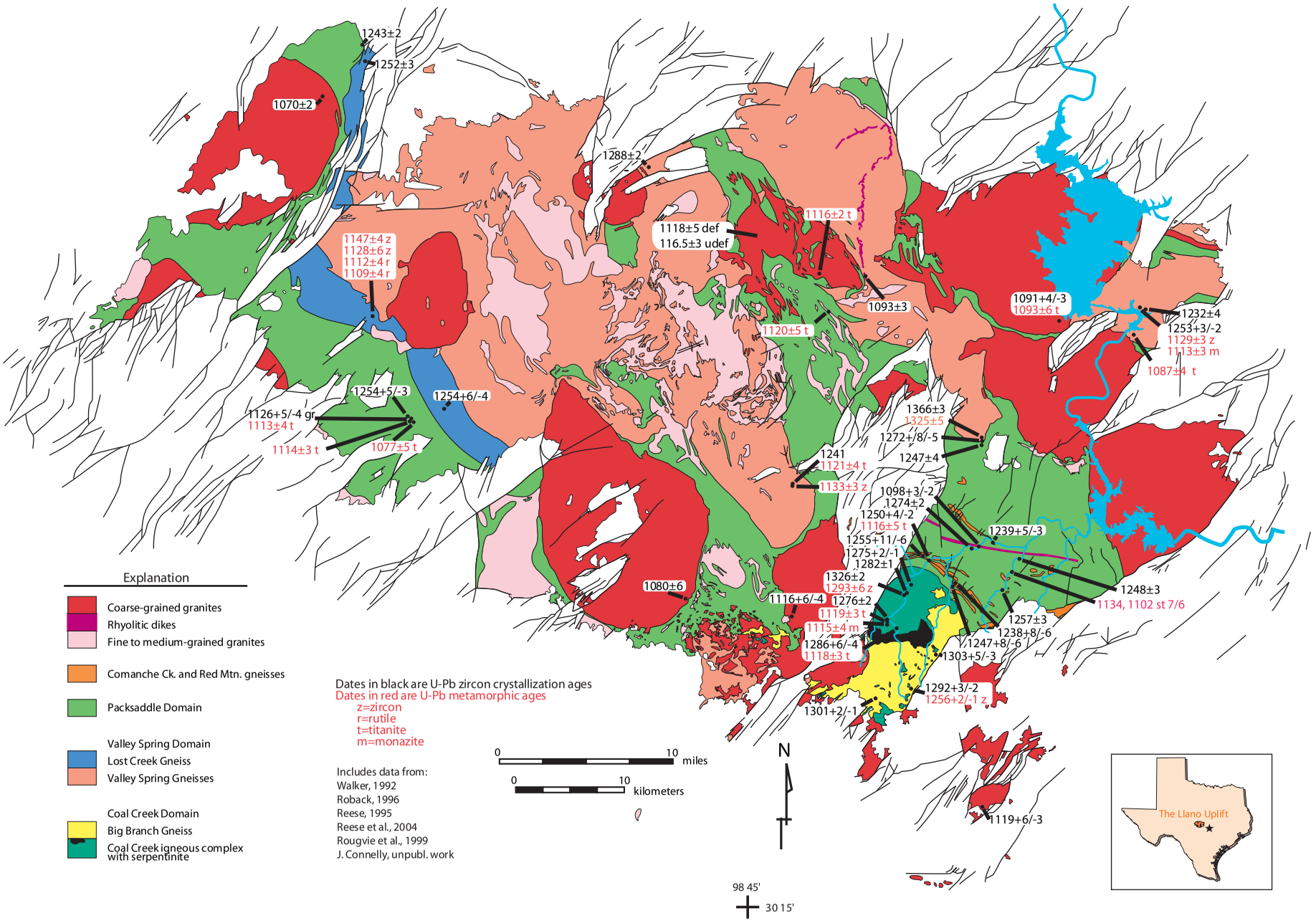

Figure 1. Geologic map of Llano Uplift (after Barnes, 1981), central Texas (see cover) with protolith and metamorphic ages.

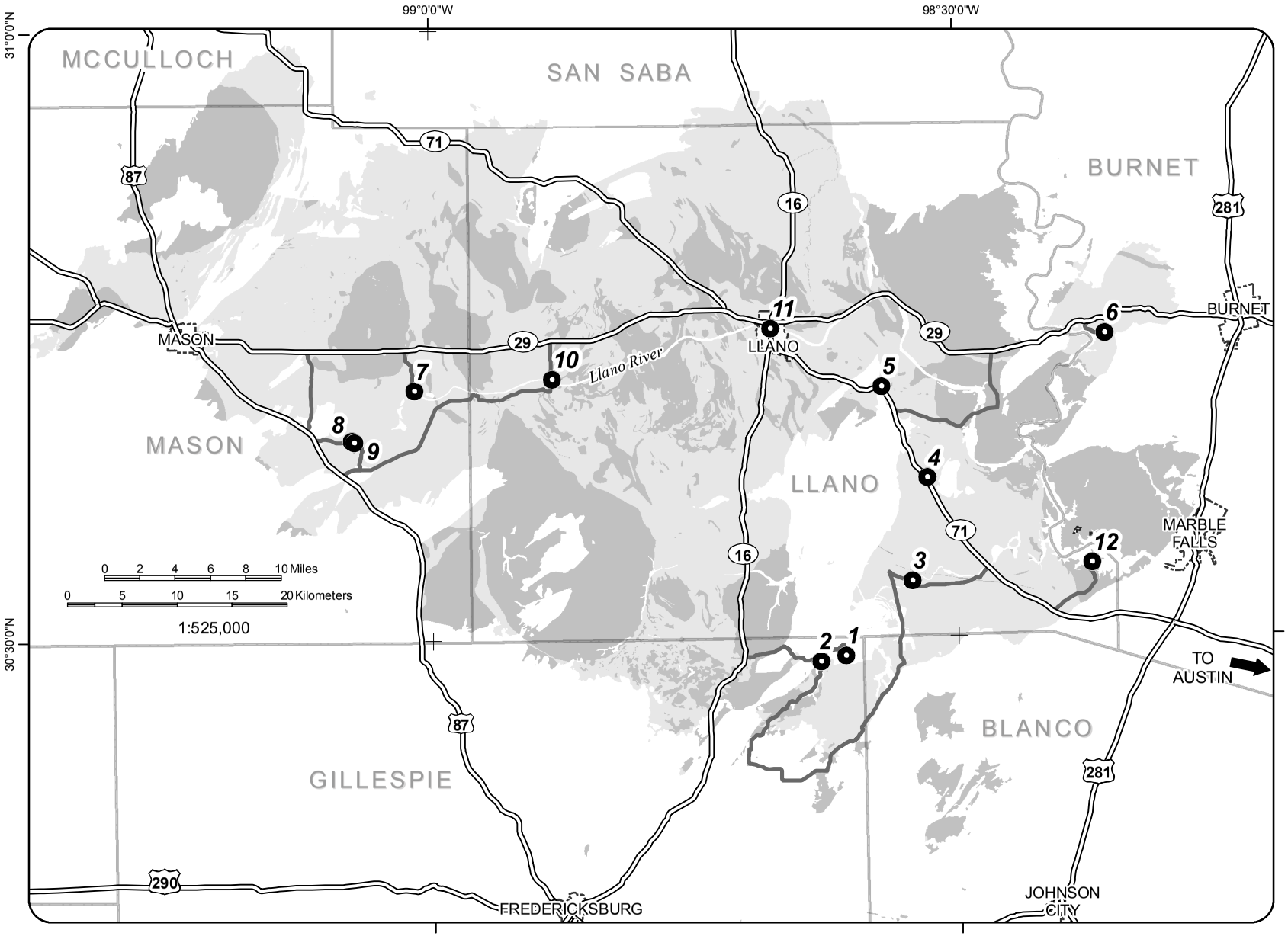

Figure 2. Field trip stops, by number. Precambrian rocks are shaded; darker tone is granite, lighter tone is schists and gneisses.

are well preserved. These younger (1292 to 1275 Ma) bodies clearly truncate the fabric in the older gneisses, but are themselves foliated. Thus, metamorphism and deformation of

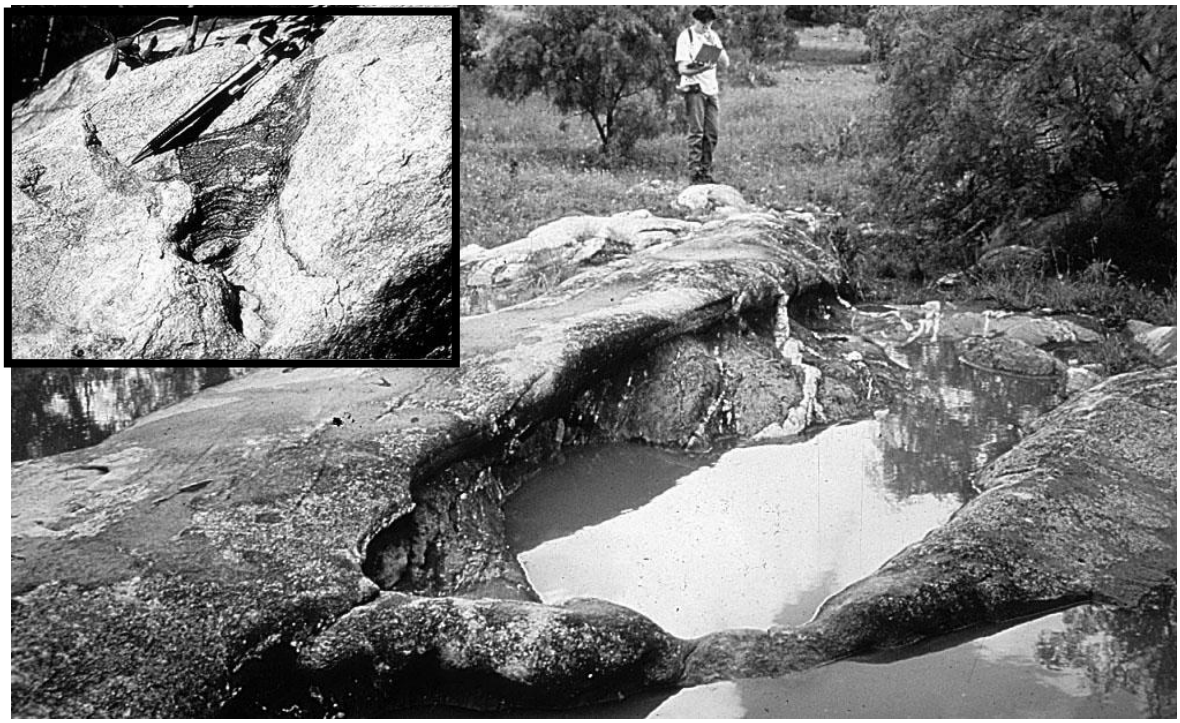

Figure 3. Outcrop showing intrusive relationship between older Big Branch Gneiss and younger tonalites of the Coal Creek igneous complex. Note an earlier foliation in the Big Branch Gneiss is truncated by the younger tonalites; see inset of xenolith of Big Branch Gneiss in younger tonalite.

gray, tonalitic gneisses occurred between 1292 and ca 1301 Ma. A younger metamorphism of the domain is directly dated at 1256 Ma (U/Pb metamorphic zircon). Both the intrusive complex and the Big Branch Gneiss are cut by mafic and felsic dikes. The igneous complex also contains gabbros, amphibolites, mafic schists, and minor talc-rich and serpentinite bodies. Sm-Nd isotopic data (Roback et al., 1995, Whitefield, 1997; Patchet and Ruiz, 1989) yield older model ages (1.4 to 1.68 Ga) for the Coal Creek domain than for most granitic gneisses outside the Coal Creek domain (1.23 to 1.48 Ga). Post-tectonic granites cutting the Coal Creek domain also yield older model ages (1.33 to 1.43 Ga) than those cutting the other domains (0.97 to 1.34 Ga) (Whitefield, 1997). Common Pb also shows a distinctly different signature from the granitic and metasedimentary domains to the north. The Coal Creek domain is only observed in the southeastern portion of the uplift.

The northern boundary of the Coal Creek domain is the Sandy Creek shear zone, a 2-3 km wide mylonite zone containing granitic (Red Mountain gneiss) to quartz monzonitic (Comanche Creek gneiss) sills and fine-grained felsic units (leptites) ranging in age from 1255-1238 Ma (Walker, 1992; Roback, 1996; Whitefield, 1997). The degree of mylonitization varies from protomylonitic to ultramylonitic within these units.

Packsaddle Domain. Supracrustal rocks of the Packsaddle domain in the eastern uplift consist of 1274-1243 Ma, metamorphosed volcanic, volcanoclastic, and sedimentary rocks interpreted to represent a marine basinal sequence (Reese et al., 2000) with a shallow-water, continental-margin depositional environment for the rocks closest to the Valley Spring domain (Reed et al., 1996; Mosher, 1998). Rocks nearest the Sandy Creek shear zone have under gone complete transposition precluding determination of many protoliths and of any original contact relationships. Deformation intensity (but not complexity) decreases northward away from the zone. More units have apparent igneous protoliths in the south near the boundary with the Coal Creek domain, and metasedimentary units (marbles, calc silicates, graphitic schists, quartzites) become dominant northward near the Valley Spring domain. In the eastern uplift, granitic sills, ranging in age from 1255 to 1238 Ma, intrude the supracrustal rocks and are affected by the polyphase deformation; an undeformed, regionally extensive rhyolitic dike dated at 1098 Ma crosscuts all structures (Walker, 1992; Roback, 1996; Whitefield, 1997). At the northern boundary of the Packsaddle domain, a ductile shear zone places Packsaddle metasedimentary and metavolcanic rocks on granitic gneiss of the Valley Spring domain (Reese, 1995; Zumbro, 1999; Mosher et al., 2004). In the western uplift, rocks of the Packsaddle domain consist of interlayered amphibolites, felsic gneisses, pelitic schists and minor calc silicates, and the few dated units yield similar ages (e.g. 1253 +5/-3 Ma; Roback et al., 1999; Hunt, 2000).

Valley Spring Domain. The Valley Spring domain consists of 1288–1232 Ma plutonic and supracrustal rocks (with one older gneiss dated at 1366 ± 3 Ma) interpreted as a continental margin arc, terrigenous clastics formed on Laurentia, and some older continental basement (Mosher, 1998; Zumbro, 1999; Reese et al., 2000). The domain consists dominantly of quartzofeldspathic gneisses and migmatites, with minor intercalated marble, mafic and pelitic schists, amphibolite and metagabbro (Barnes, 1981). Migmatites are common in the western uplift and in the structurally lower parts of the Valley Spring domain in the eastern uplift. In the eastern uplift, the structurally uppermost Valley Spring domain is an intrusive complex juxtaposed with the Packsaddle domain along a ductile shear zone, and structurally lower parts contain sedimentary and perhaps volcanic rocks intermixed with plutonic rocks (Zumbro, 1999; Mosher et al., 2004). In the western uplift, both metasedimentary and igneous protoliths have been identified. There, the Valley Spring and Packsaddle contact is intruded by a granitic intrusion dated at 1252-1254 Ma that forms the majority of the unit mapped as Lost Creek Gneiss (Hunt, 2000).

Deformation

Rocks of the Packsaddle and Valley Spring domains across the uplift have undergone five phases of outcrop to regional scale folding resulting in the formation of five metamorphic foliations and several stages of extension (Nelis et al, 1989; Carter, 1989; Mosher, 1993, 1998; Hunt, 2000; Reese and Mosher, 2004; Mosher et al., 2004; Levine, 2005). The regionally dominant foliation is a composite S1/S2 foliation that can be locally distinguished in the hinges of F2 folds. Late-stage extension and shear zones are locally developed.

The eastern uplift is characterized by early ductile shear zones, both between and within lithotectonic domains, followed by polyphase folding. Tectonic transport, as indicated by asymmetry of porphyroclasts in mylonites and fold vergence, is towards the northeast (Nelis et al, 1989; Reese, 1995; Reese and Mosher, 2004). In the western uplift, no mylonites have been observed and the deformation is more distributed. Structural stacking of lithotectonic domains is opposite that of the eastern uplift and vergence is generally to the southwest (i.e. the Valley Spring domain is structurally highest in the western uplift and lowest in the eastern uplift).

In the eastern uplift folds generally trend southeast and foliations strike northwest and are commonly southwest-dipping, except where reoriented by younger folds. F_4 folds, in contrast, are generally E-trending with E-striking foliations, although fold axes are reoriented by F_5 folds. In the western uplift, most fold generations generally trend ESE with north- to northeast-dipping foliations, and F4 folds trend northeast. Leucosomes parallel to the first three foliations are common in both the Packsaddle and Valley Spring domains in the western uplift and only at the deepest structural levels in the Valley Spring domain of the eastern uplift, indicating partial melting during deformation. In the Packsaddle domain of the eastern uplift, five crosscutting metamorphic foliations are preserved in delicate, crenulation cleavages that formed synchronous with metamorphic differentiation. In general the plutonic complex of the Coal Creek domain is less penetratively deformed, however, mafic schists within the domain show a deformational history that is similar to the rest of the uplift. The dominant foliation affecting the plutonic complex is parallel to and can be traced into the regional S2 foliation in the Packsaddle domain.

Late stage to post-contractional N-S extension is locally observed in the eastern uplift (Carter et al., 1993). Structures associated with this extension include boudinage, fibrous quartz veins and sheets, and extensional crenulation cleavages with associated biotite differentiation (Reese, 1995; Reese and Mosher, 2004). In the western uplift, late stage shear zones and boudinage commonly are associated with granitic material indicating the presence of melt during deformation (Hunt, 2000; Levine, 2005).

Metamorphism

Metamorphic rocks in the Llano Uplift record a complex polymetamorphic history (Carlson et al., 2007). High-pressure (HP) metamorphism (610–775°C at 1.4–2.4 GPa) is recorded by eclogites, with the highest pressures in the western uplift. A subsequent moderate-pressure (MP) metamorphism (~700°C at ~0.7 GPa) was synchronous with the regional deformation across the uplift. A later, low-pressure overprint (525–625°C at 0.3 GPa) is associated with the late-stage syn- to post-tectonic granites.

The high-pressure metamorphism is recorded in relict eclogitic assemblages in the western and central uplift (Wilkerson et al., 1988; Carlson and Johnson, 1991; Gobel, 1992; Carlson et al., 2007). The western uplift mafic bodies yield temperatures of ~775 °C and pressures that decrease from ~2.4 GPa to ~1.6 GPa, indicating emplacement to a depth of ~70 km that decreased during exhumation to ~50 km. The central uplift bodies yield minimum pressures of ~1.4 GPa at temperatures near 650 °C (Carlson et al., 2007),

indicative of depths of 42 - 46km. Garnet cores formed at amphibolite facies and rims at eclogite facies, indicating increasing depths with time.

The medium-pressure dynamothermal metamorphism produced fairly uniform temperatures near ~700 °C (Carlson et al., 2007). In the Valley Spring domain of the western uplift and in the eastern uplift at deepest structural levels, deformation at uppermost amphibolite facies conditions was associated with partial melting during F_1/S_1-F_3/S_3, with sillimanite as the stable aluminumsilicate. In the Packsaddle domain of the eastern uplift, end-member-Fe staurolite that grew between S_2 and S_3 records temperatures of ~700°C at ~0.7 GPa (Carlson and Nelis, 1986; Carlson and Reese, 1993, 1994), indicating exhumation to depths of ~23 to 26 km. In the Coal Creek domain, relict metamorphic enstatite and forsterite in a later reserpentinized harzburgite record temperatures of ~700°C (Gillis, 1989). Temperatures decreased somewhat after F_3/S_3 (Reese and Mosher, 2004; Mosher et al., 2004; Levine, 2005).

Regional dynamothermal metamorphism has been overprinted by a mid-amphibolite facies metamorphism throughout the uplift. Isotopic evidence indicates that static reheating and hydration is genetically related to "post-tectonic" granite pluton emplacement (Bebout and Carlson, 1986). Although this metamorphism is generally "static", F_5 folds are temporally related to the earliest of the late granite plutonism. Temperatures ranged from 525–625^{o}C at ~0.3 GPa (Wilkerson et al., 1988; Carlson and Schwarze, 1993; Carlson, 1998; Letargo et al., 1995).

Late-stage Plutonism

Roughly oval to circular, coarse-grained, pink K_2O-rich granite plutons (termed Town Mountain Granite) intrude the metamorphic rocks across the entire uplift. These upper mesozonal to low epizonal plutons (Hutchinson, 1956) have been dated at 1119-1070 Ma (Walker, 1992; Reed, 1999). Granites have a juvenile Nd signature and geochemistry compatible with combined crustal and depleted mantle sources (Smith et al., 1997). Sm-Nd isotopic data yield model ages of 0.97 to 1.34 Ga for most of the uplift with older model ages of 1.33 to 1.43 Ga for those intruding the Coal Creek domain (Packett and Ruiz, 1989; Whitefield, 1997). Finer-grained granites, previously considered younger, are not distinctly different from the Town Mountain Granites chemically and appear at least locally to be cogenetic with the coarser-grained bodies. The oldest plutons are late syntectonic. Ductile shear zones locally cut the older granites with deformation ranging from proto- to ultra-mylonitic (Grape Creek pluton dated at 1119+6/-3 Ma; Reed et al., 1995). One large sheet-like pluton, the Wolf Mountain pluton (dated at 1118+/-5), is folded by an F5 fold and locally contains an axial planar tectonic fabric as well as a magmatic fabric parallel to the pluton margins. This pluton is cut by an undeformed medium-grained granite dated at 1116.5 +/-3 Ma, indicating deformation ceased in this part of the uplift by this time (Reed, 1999). Numerous coarse grained to pegmatitic granites with apparent Town Mountain affinities are folded by late-stage folds and/or boudinaged, including one dated at 1126+5/-4 (Roback et al., 1999).

Timing of metamorphism and deformation

Timing of metamorphism and deformation is constrained between 1147 Ma and 1115 Ma. The early high-pressure metamorphism is dated by three U/Pb zircon ages and one Lu-Hf garnet-rutile age at 1147–1128 Ma in the western uplift and 1133–1134 Ma in the central and eastern uplift (Carlson et al. 2007). The regional deformation and medium-pressure metamorphism in the eastern uplift is dated at 1129 ± 3 Ma by a U/Pb metamorphic zircon age for mafic rocks in the Valley Spring domain (Mosher et al., 2004), although it could possibly record the earlier high-pressure metamorphism. Exhumation of the high-pressure rocks appears to have been rapid. The low-pressure metamorphism is associated with the late-stage granite plutons, and metamorphic titanite, rutile and monazite yield ages of 1115 +/-6 Ma. The oldest 1119–1118 Ma plutons are syn-tectonic to F5. Although an undeformed granite dated at 1116.5 +/-3 Ma cuts the folded (F5) Wolf Mountain pluton, other plutons dated at 1116 Ma show some signs of deformation. Plutons younger than 1093 Ma are undeformed internally, although country rock around plutons as young as 1080 Ma was deformed during intrusion (Reed, 1999). An undeformed, regionally extensive rhyolitic dike dated at 1098+3/-2 Ma cross cuts all structures in the southeastern uplift (Nelis et al., 1989; Walker, 1992)

Tectonic Evolution

The Llano uplift of central Texas exposes the core of a Mesoproterozoic orogenic belt that formed along the southern margin of Laurentia during Grenville time. Orogenic activity in central Texas was long-lived, spanning at least 250 Ma and culminated with the collision of a long-lived (60 Ma) island arc terrane with a continental block (Valley Spring domain) that may represent the southern margin of Laurentia (Mosher, 1998). The presence of medium-T eclogites, indicative of A-type subduction, suggests collision of a continental block as well. Subduction polarity leading to collision must have been southward as no arc-related activity is recorded in the Llano uplift after ~1232 Ma.

Mosher et al. (2008) have proposed a new model for the collisional part of the tectonic history that explains uplift and exhumation of high-P eclogitic rocks, emplacement of ophiolitic rocks, and subsequent late stage to post-collisional plutonism (Fig. 4). This model reconciles

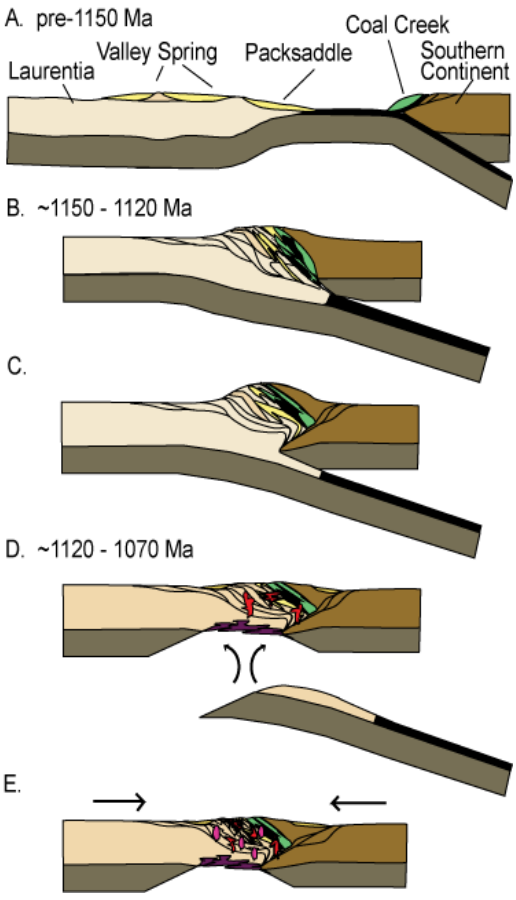

Figure 4. Tectonic model for Grenville orogeny along southern margin of Laurentia, showing evolution of the Llano Uplift (from Mosher et al., 2008).

differences in structural stacking, apparent tectonic transport, and deformation conditions between the eastern and western portions of the uplift. The eastern uplift records continent-arc-continent collision whereas the western uplift records continent-continent collision; the two regions also expose different crustal levels in the orogen. In the model, subduction with southward polarity results in collision of an exotic arc with Laurentia, during which ophiolitic rocks are emplaced, the intervening basinal sediments are telescoped, and a southern continent overrides the arc and margin of Laurentia. The model further proposes that convergence led to subduction of the Laurentian margin, resulting in high-P metamorphism, but buoyancy forces due to subduction of continental crust under the southern continent resulted in uplift and retrotransport away from Laurentia. Slab breakoff resulted in upwelling of the asthenosphere, leading to intrusion of juvenile granitic plutons. Subduction along strike caused continued contraction that waned with time.

DAY 1

We will make a transect across the eastern uplift from south to north looking at the three distinct lithologic/structural domains and the polyphase deformation and metamorphism within them. Figure 5 shows the structural and age relationships between the lithotectonic domains and the tectonic nature of the contacts. The first stops are in the Coal Creek domain to look at relationships within the island arc complex. This domain has been subdivided into two parts (see cover map and Figs. 5 and 6): 1) an older Big Branch Gneiss (1301 - 1326 Ma) that crops out primarily south of the serpentinite and locally north of the serpentinite, where it is intruded by 2) a mafic igneous complex dated at 1275-1292 Ma. We will concentrate on the Coal Creek domain north of the serpentinite where the relationships within the igneous complex can be easily viewed. Note that at all stops, igneous relationships are well preserved despite later deformation, in marked contrast to the Packsaddle domain. .

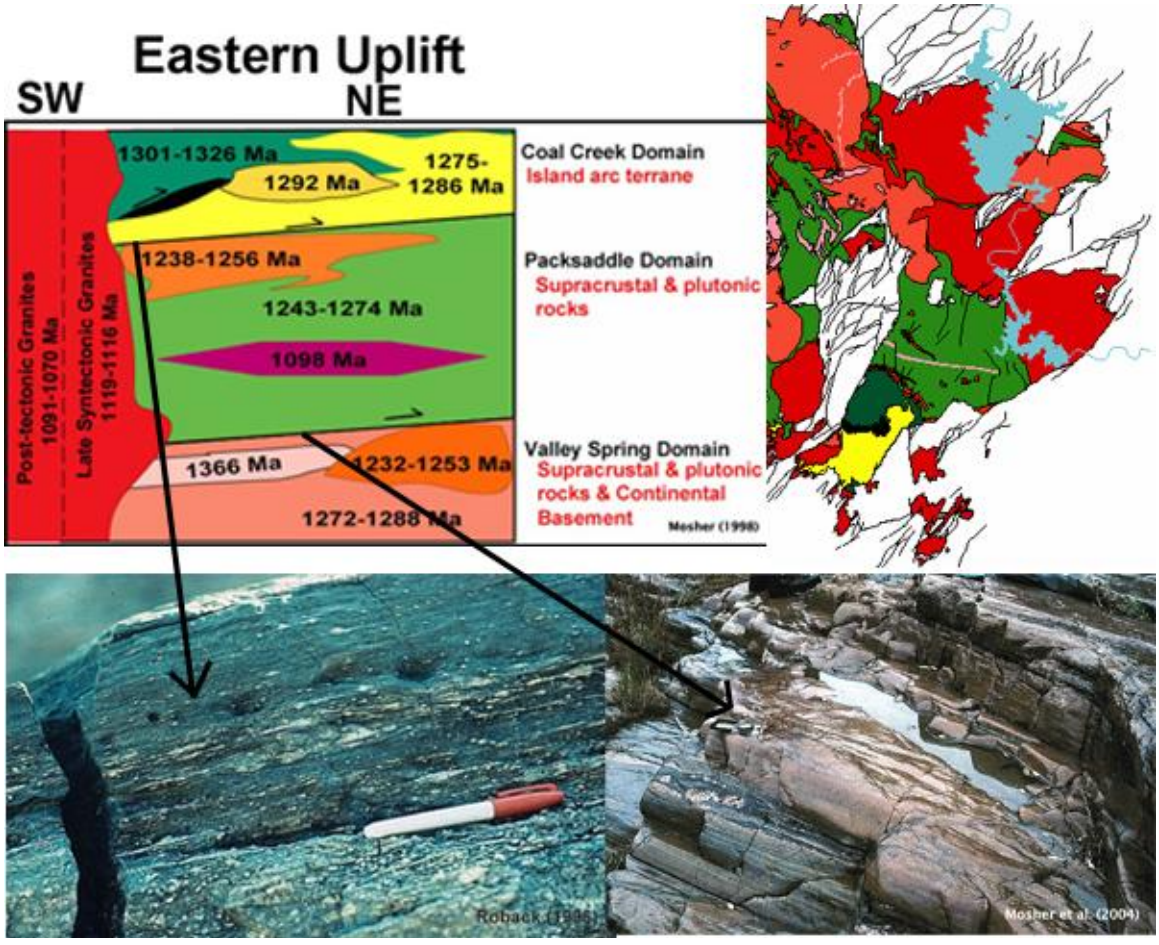

Figure 5. Structural column (upper left) showing the relationships between lithotectonic domains in the eastern uplift (after Mosher, 1998) and generalized geologic map of eastern uplift with the same color scheme (upper right). Photographs show mylonites in ductile shear zones separating the domains.

For the rest of the day we will work our way northwards. The first stop within the Packsaddle domain is in generally orthogneissic units near the boundary with the

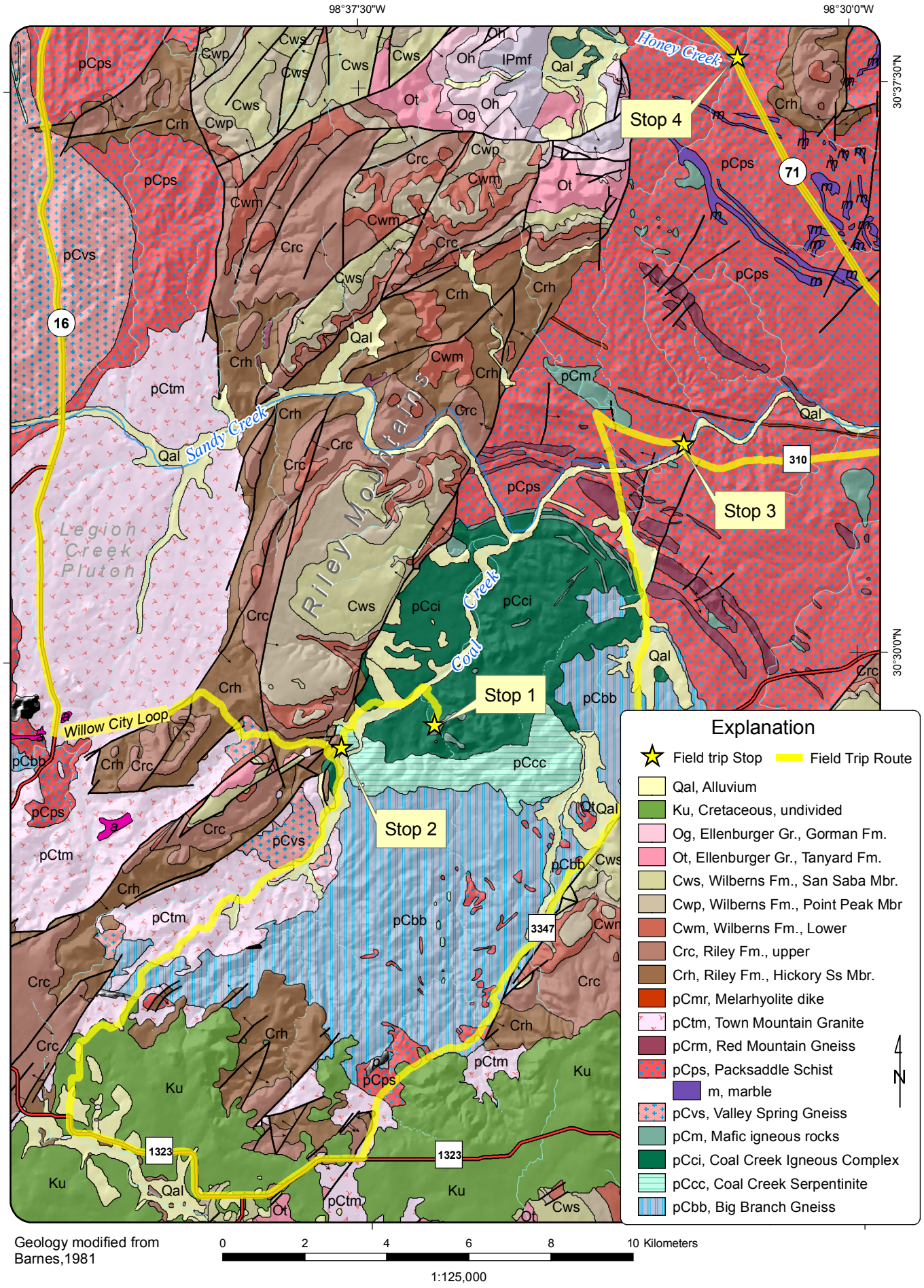

Figure 6. Geologic map of the southeastern Llano uplift, showing Stops 1-4.

Coal Creek domain. At the second we will briefly look at graphitic schists with sedimentary protoliths near the boundary with the Valley Spring domain. At the first stop within the Valley Spring domain we will examine one of the relict eclogite bodies and its relationships to the surrounding felsic gneisses. The second Valley Spring stop will be in the gneissic units at the structurally lowest levels of the domain where mixed protoliths and migmatites are exposed. For stop locations, see Fig. 2

PLEASE NOTE: All but the last stop are on private property. **Permission must be obtained to visit these stops!** We have obtained special permission from landowners to visit several of these key stops that are not usually accessible to groups. If you wish to visit these stops, please contact Sharon Mosher (e-mail: mosher@mail.utexas.edu) for further information.

From the Lone Star Inn in Llano, turn right on Hwy 29 and drive to intersection with Hwy 16. Turn right (south) and drive across Llano River. From the south side of the Llano River bridge, drive 18.9 miles south on Hwy 16 to left turn on Willow City Loop. After the left turn on Willow City Loop, drive another 4.9 miles to an intersection with Willow City – Click Road and turn right. Continue on this road for 2.0 miles and turn right onto Big Branch Road. Drive another 0.7 miles to the Smith ranch.

Stop 1: Ensimatic arc rocks of the Coal Creek igneous complex, Coal Creek Domain, Smith Property, Big Branch Creek, Gillespie County.
The following description is by M. A. Helper, modified from Roback (1996; in Mosher, 1996). ***N.B. This stop is on private property. Permission must be obtained to visit this site.***

This stop (Figs. 2 and 6) examines lithologies, intrusive relationships and fabrics within a portion of the Coal Creek Domain (CCD), the oldest and structurally highest terrane of the Llano uplift. Long regarded as distinct for its more mafic character and the presence of metaserpentinite, talc schist and allied metasomatic rocks (e.g. Barnes, 1945; 1978; McGehee, 1979), this southeast-most region of the Llano uplift preserves fragments of ensimatic arc basement and oceanic crust that were accreted to the Laurentian margin at ~1150-1120 Ma (Garrison, 1981a, b; Roback, 1996; Mosher, 1998; Mosher et al., 2008). At this stop, we examine the younger arc component (Coal Creek Igneous Complex, Fig. 6) of the CCD: a low-K intrusive suite of 1292-1275 Ma hornblende gabbro, tonalite, diorite, and granodiorite. Intrusive relationships and primary textures are well preserved, as are overprinting fabrics. An older component, a suite of 1326-1301 Ma gneissic tonalites, diorite, amphibolites and migmatites (the Big Branch Gneiss of Roback, 1996a and Fig. 6) that is country rock to the igneous complex, is not present at this locality. Metaserpentinite is the focus of Stop 2.

The area of this stop was mapped in detail as part of a larger structural study by Gillis (1989) and was reexamined and reported on by Roback (1996; Roback in Mosher, 1996), whose work provides the U/Pb zircon ages cited below.

Park at the residence, proceed southward around the fenced yard and enter the drainage of Big Branch Creek. Walk north (downstream) for approximately 0.3 km to

where a telephone line crosses above the creek. We will traverse from north to south, examining the rocks as we backtrack upstream. Immediately east of the house in the creek is the midpoint of a gradational contact between dominantly mafic rocks to the south and more felsic rocks to the north (see Garrison, 1979; Gillis, 1989). This transition was once regarded as the boundary between Big Branch Gneiss to the north and Packsaddle Schist (Click Formation) to the south, and is shown on most published maps as such. As will be evident from all outcrops, rocks on both sides of the transition, though foliated, are not gneissic and preserve many aspects of their primary intrusive character. Moreover, U-Pb dates of all lithologies here are markedly younger than truly gneissic Big Branch Gneiss to the south and east (Fig. 6). These differences in age, texture and fabric, which can be recognized throughout the CCD, are the basis for revisions to the original mapping and for delineation of the Coal Creek igneous complex (Reese et al., 2000).

Proceeding upstream, four rock types common to the area are encountered. From oldest to youngest these are: hornblende plagioclase metagabbro and amphibolite; leucocratic biotite granodiorite; medium gray, biotite tonalite; and straight-walled, mafic dikes. Relative ages are demonstrated by intrusive relationships along the creek. Xenoliths of hornblende gabbro/amphibolite are present within the more felsic plutonic rocks. Within at least one outcrop, biotite tonalite intrudes granodiorite. Several localities show straight walled mafic dikes cutting the other rock types. All of these lithologies share a common penetrative foliation. Younger, less well foliated, fine-grained granitic dikes cut all rock types.

Locality A: The first outcrops in the creek bed immediate upstream of the telephone line are medium-grained, gray, foliated biotite tonalite that contains included angular, blocky to tabular pieces of foliated fine- to medium-grained amphibolite, both of which are cut by fine-grained foliated leucocratic biotite granodiorite (Fig. 7). Biotite tonalite in this outcrop has a U/Pb zircon crystallization age of 1276$\pm$2 Ma. An additional, lithologically similar sample from approximately 4 km to the north yielded an age of 1275+2/-1 Ma. These tonalites are a volumetrically important component of the CCD.

The other two lithologies have not been dated here. Roback (1996) and Gillis (1989) considered the angular mafic blocks in these outcrops to be xenoliths of hornblende metagrabbro and amphibolite, lithologies that are abundant upstream (see below) and elsewhere in the CCD. An alternative explanation for some of these inclusions is that they represent mafic magma that invaded the tonalite after it had crystallized. This is perhaps suggested by blocks that are partially rimmed or separated from the including tonalite by quartz-feldspar selvages that are contiguous with veinlets that cross cut the mafic inclusions (Fig. 8). These veinlets and selvages are texturally and modally different from the biotite tonalite. By this explanation, these may represent anatexis of the surrounded tonalite during intrusion of a mafic magma that produced the inclusions.

Lithologies at all localities at this stop contain a high temperature, east to southeast dipping foliation (S2; see Gillis, 1989) that is the product of dynamothermal

metamorphism at upper amphibolites facies. This dominant fabric is shared by all domains of the uplift and is thought to have formed during accretion of the CCD along the Sandy Creek shear zone.

Localities B and C: About 30 m upstream from Locality A (site of Locality B) and again at about 120 m beyond (Locality C), ~ 1 meter thick, south-dipping, fine-grained, garnetiferous, granitic dikes form prominent ledges. Within the dikes, coarser quartz and K-feldspar define a crude foliation that is locally ptygmatically folded. These veins must have formed during a high temperature metamorphism and may be minimum partial melts of the dike. The granitic dikes cut northward trending, fine-grained, dark green, ~ 1 - 1.5 meter thick mafic dikes. Similar mafic dikes are common throughout the CCD and are herein referred to as straight-walled dikes. At both localities, straight-walled dikes intrude medium-grained, gray tonalite. A well developed foliation cuts both the tonalite and straight-walled dike and is parallel to the foliation in the granitic dike. Relative ages, from oldest to youngest, at both localities are: 1) biotite tonalite, 2) mafic straight-walled dike, 3) garnetiferous granitic dike.

Figure 7. Mafic inclusion in biotite tonalite at locality A. Left of the pen, an apophyse of the tonalite cuts the mafic inclusion, consistent with the interpretation that some mafic inclusions are xenoliths.

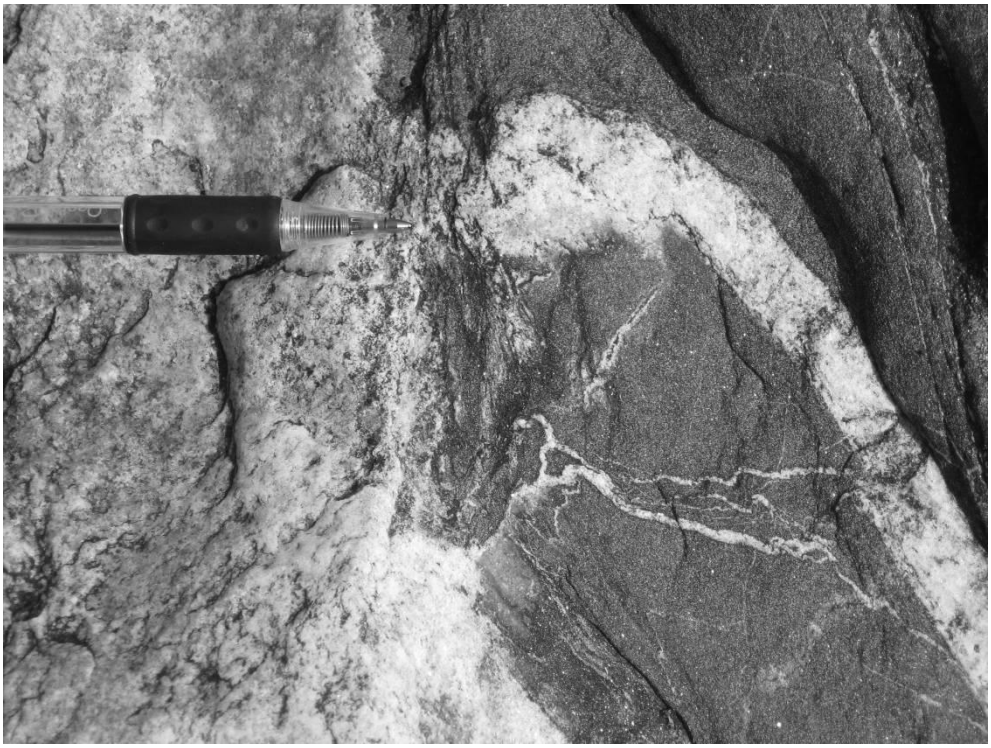

Figure 8. Plagioclase-quartz selvage (beneath pen) at the margin of a mafic inclusion, and veins and veinlets of the same within an inclusion at locality A. These textures are consistent with the inclusions having caused partial melting of the host tonalite, requiring that they are younger than the tonalite and are thus not xenoliths.

Zircon from the garnetiferous granitic dike farthest upstream (locality C) show disturbed or mixed isotopic systematics and do not define a U/Pb discordia trajectory. $^{207}Pb/^{206}Pb$ ages range from ca 1280 Ma to 1290 Ma, which are minimum ages of at least a part of the dated zircon population. Because the dike intrudes tonalite dated at 1276 Ma, it must be younger. The dated zircons are thus probably xenocrystic, perhaps derived from the 1326-1301 Ma basement gneisses of the CCD. Titanite from the same dike is concordant at 1120 Ma, as is monazite (1115 $\pm$ 3 Ma) from the garnetiferous granitic dike at locality B. Both dates are within the age range of the late-stage, voluminous Town Mountain plutonic suite (stop 12, Day 2) and associated static amphibolite to greenschist facies metamorphism and are thus interpreted to record this thermal event.

The peraluminous, granitic composition of the garnetiferous granitic dikes differs greatly from the low-K and more mafic rocks of the CCD; Pb isotopic signatures of the two are also different (Roback, unpublished data), indicating that these dikes, which by field relationships are the youngest intrusions in the CCD, are probably not part of the CCD igneous complex. Pb from the CCD has consistently higher $^{207}Pb/^{204}Pb$ values for given $^{206}Pb/^{204}Pb$ values. $^{208}Pb/^{204}Pb$ values for all rocks in the uplift overlap and document a wide, long-term range of Th/U ratios. Pb from the granitic dike at locality C plots well within the field of non-CCD rocks. Pb from the dike at locality B plots

intermediate between the CCD and non-CCD fields, probably reflecting contamination by CCD rocks, as also indicated by the U-Pb zircon data described above for this dike.

Although superficially similar to other foliated mafic rocks in the CCD, straight-walled mafic dikes like those at locality B and C comprise a chemically, isotopically and temporally distinct suite. The absolute age of the dikes is unknown, but by field relationships they are the youngest mafic rocks within the CCD. Many show a preferred orientation approximately 30° from north. Others follow the strike of the dominant foliation, making them very difficult to distinguish from older mafic rocks. Compared chemically to other mafic rocks of the CCD, straight-walled dikes contain significantly higher TiO_2 (1.4 to 2.2 wt % vs. <1.2 wt %, with most <0.8 wt %), Zr and Y. Chondrite-nomalized REE patterns for all high Ti CCD dikes are flat (avg. La/Y = 1.3); low Ti dikes, display negative slopes (avg. La/Y = 4.6). These chemical differences led Roback (in Mosher, 1996) to consider these dikes genetically distinct from the CCD igneous complex.

Locality D: Continue upstream past the residence. Notice that tonalitic plutonic rocks become less abundant and hornblende gabbro and amphibolites predominate. Approximately 200 meters upstream from the house, igneous textures are well preserved in the gabbro. Relict igneous layering is preserved in one outcrop here. Also notice variable textures and compositions of the gabbro.

Hornblende gabbro from these outcrops gives a U-Pb zircon crystallization age of 1286 +6/-4 Ma. Titanite from the same sample is concordant at 1120±3 Ma. This age is similar to U-Pb ages of titanite and rutile described above and interpreted similarly - these ages reflect metamorphism during emplacement of the Town Mountain plutonic suite.

Sm-Nd isotopic studies of these and other lithologies within the CCD corroborate field evidence for definition and delineation of the CCD and emphasize fundamental geochemical differences between the CCD and the rest of the uplift. CCD rocks have T_{DM} that range from 1.4 to 1.68 Ga, with many around 1.5 Ga, and $eNd_{(t)}$ values of +2 to +4. Non-CCD metamorphic rocks have younger T_{DM} ranging from 1.23 to 1.48 and $eNd_{(t)}$ generally above +3.5. These data point to distinctly different sources components, either in mantle, crust or both, for formation of CCD and non-CCD crust in the uplift.

Stop 2: Serpentinite Quarry.
The following description is modified from Mosher (1996). ***N.B. This stop is on private property. Permission must be obtained to visit this site.***

The Coal Creek Serpentinite is a tabular shaped, south-dipping body, approximately 6 km long and 500 m to 2.3 km wide. It is intruded by numerous thin metabasaltic dikes that show metasomatic alteration zones at their margins. The serpentinite is composed of lizardite, secondary veins of chrysotile, and accessory magnetite, tremolite, talc, chlorite, and relict chromite in layers. Massive samples contain lizardite mesh texture pseudomorphing olivine and pyroxene and minor metamorphic amphibole. Rare samples contain olivine, orthopyroxene, and anthophyllite, suggesting the body was originally harzburgite (Garrison, 1979; 1981a and b).

The serpentinite record a complex history of multiple serpentinizations, metamorphisms and deformations (Gillis, 1989). Based on the data presented below, Gillis and Mosher (1988) suggest the serpentinite was tectonically emplaced as a harzburgite and partially to completely serpentinized during emplacement. The unit then underwent regional metamorphism and deformation along with the country rock, during which it was deserpentinized. During emplacement of the granites, static metamorphism resulted in growth of metamorphic anthophyllite, and then as temperatures waned, fluids associated with the granites caused reserpentinization.

- The present-day serpentinite most likely formed during granite intrusion while temperatures were waning. Isotopic data (Delta ^{18}O, +5.219 to +6.846 and delta D, -76 to -81) suggests equilibration with magmatic water at 300-400°C, but not seawater or present-day meteoric water (Garrison, 1979).

- The serpentinite shows a well-developed relict foliation defined by aligned elongate pseudomorphs of olivine and pyroxene (Gillis, 1989). Blackwall zones between both basaltic dikes and country rock and the serpentinite are composed of talc, tremolite, and Mg-chlorite that are aligned and define a well developed foliation that parallels and is continuous with the foliation with in the serpentinite. These relationships indicate that some serpentinization occurred earlier, prior to or synchronous with the formation of the foliation.

- The outermost 10 m of the serpentinite body at its southern margin is comprised of highly sheared chlorite-rich rocks with tremolite and magnetite slickensides, suggesting that early serpentinization occurred during emplacement of the Coal Creek body.

- The ultramafic body was affected by regional metamorphism and reached temperatures of about 700-750°C. These metamorphic conditions are supported by the compositions of the relict olivine ($Fo_{93.5}$ - $Fo_{94.0}$) and orthopyroxene ($En_{92.2}$ -$En_{93.7}$), very high Cr/Cr+Al and low Mg/Mg+Fe ratios, NiO content, presence of metamorphic anthophyllite and chlorite and chromite not in equilibrium with magnetite (Garrison 1979). Although these data are consistent with regional metamorphism of the original harzburgite, they are more consistent with deserpentinization.

- The serpentinite contains a relict foliation and is folded similar to the surrounding country rock, suggesting it shared a similar deformational history (Gillis, 1989).

- Evidence for reserpentinization includes radial sprays of chlorite and rare tremolite in blackwall zones that overgrow the foliation and two generations of crenulations, partial replacement of anthophyllite and orthopyroxene by talc in the serpentinite, and psuedomorphing of most minerals by serpentine, including radial sprays of anthophyllite.

This stop shows the general characteristics of the Coal Creek Serpentinite, but not all of the relationships outlined above. Exposure varies depending on the amount of quarrying and erosion.

Return to Willow City Loop and turn left. Drive 5.2 miles to the junction with CR 1323. We will stop at a pullout along this road to discuss the regional geology and association with topography. At this junction continue straight, another 5.4 miles and turn left onto Althaus-Davis Road. Drive 3.7 miles along Althaus-Davis Road to cattle guard at Blanco/Gillespie county line.

County Line outcrop: On right is the agmatite outcrop of Roback (1996). Angular to rounded mafic amphibolitic blocks yield a metamorphic zircon age of 1256 +2/-1 Ma, whereas the light-colored, foliated leucotonalite which surrounds them yields a crystallization age of 1292+3-2 Ma. Numerous thin dikes emanate from the tonalite and intrude the mafic blocks. This outcrop is now overgrown and the landowner does not want groups stop.

Continue 4.2 miles and turn left turn onto CR 309, also known as Lynn Harden Road. As you pass Red Mountain on your right, you have crossed from the Coal Creek domain into the Packsaddle domain and are within a 2-3 km thick shear zone, the Sandy Creek Shear zone. Unfortunately landowner changes preclude a stop within this zone.

Sandy Creek Shear zone: The boundary between the Packsaddle and Coal Creek domains is a zone of intense mylonitization termed the Sandy Creek shear zone (Roback, 1996). This shear zone is 2 to 3 km thick and involves abundant granitic sills that intrude rocks of the Packsaddle domain (Whitefield, 1997). The mylonites grade from protomylonites and augen gneisses at the southern shear zone margin to mylonites and ultramylonites within the shear zone (Fig. 5). Foliation generally trends NW and parallels S_2 in the rocks adjacent to the shear zone. A SW-plunging stretching lineation is defined by elongated quartz and feldspar. In thin section mylonites contain recrystallized microcline augen wrapped by biotite and fine-grained quartz and feldspar, and recrystallized quartz ribbons (Carter, 1989). Mylonitized granitic sills within the shear zone include the Red Mountain Gneiss and Comanche Creek gneiss (Reese et al., 2000) dated at 1239 +5/-3 Ma and 1238 +8/-6 Ma respectively (Walker, 1992) and a fine-grained granite sill dated at 1250 +4/-2 Ma (Roback, 1996). Together these ages constrain the age of mylonitization in the Sandy Creek shear zone to $\leq$ 1238 Ma. The Comanche Creek gneiss is granodioritic to quartz monzonitic in composition, with abundant, large, white microcline augen and biotite. The Red Mountain Gneiss is variably foliated to massive, pink to red, and granitic in composition, containing perthitic microcline, quartz, and little else.

Drive for 4.7 miles on 309, cross Sandy Creek and drive another 0.8 miles to CR 310. Turn right. Travel 1.5 miles on CR 310 to another ford of Sandy Creek. We will examine outcrops on the northwest side of the creek that were studied in detail by Nelis et al. (1989) and are further described in Reese and Mosher (2004). ***Please note this is the first time since the early 1990's that permission has been granted to visit these outcrops***

and that owner will not allow future groups access. An optional stop is also described at the White Creek crossing.

Stop 3. Sandy Creek Ford, Packsaddle domain just north of Coal Creek domain
The following description is modified from Mosher (1996) and Mosher and Reese (2004).
N.B. This stop is on private property. Permission cannot be obtained to visit this site.

The Packsaddle domain adjacent to the Coal Creek domain consists primarily of metavolcanic, metavolcanoclastic and some metaplutonic rocks, although some sedimentary units are interspersed. Reese et al. (2000) dated three felsic metavolcanic units interlayered with the metasedimentary units at 1247 +/-4 to 1257+/-3 Ma (U/Pb zircon ages). The felsic metavolcanic rock within the Packsaddle domain dated by Walker (1992) falls within this range, but a white quartz, feldspar, muscovite schist with rare piedmontite and garnet lenses from this stop near the Coal Creek domain yields 1274 +/-2 Ma age. Isotopic data of Whitefield (1997) confirms that this unit is part of the Packsaddle domain, extending the age range for this domain from 1247 to 1274 Ma.

All rocks in this part of the domain are intensely deformed and transposed. Original intrusive and contact relationships are obliterated. The prominent foliation (S_2) is mylonitic in places, and in others is a crenulation cleavage of an earlier metamorphic fabric (S_1). Wide, early mylonite zones are multiply folded by subsequent fold generations. The largest scale folds in this area are SE-plunging asymmetric F_5 folds verging to the northeast (Fig. 9). In some outcrops, it is possible to see five foliations on limbs of F_5 folds (see outcrops near ford; Fig. 10). S_1 is isoclinally folded by an F_2 fold with S_2 axial planar. Where S_1 and S_2 are parallel, they cannot be distinguished. S_2 is crosscut by three foliations defined in outcrop by differentiation of biotite. In thin section, the differentiation is parallel to limbs of crenulations. One foliation (S_4) strikes oblique to the rest, nearly east-west (Fig. 9). In many places (further down the creek), the pronounced fabric is S_3. Careful inspection shows that the foliation is a crenulation of a preexisting foliation, S_2 (that in thin section is a crenulation of an even older foliation - S_1). S_3 is folded by F_5 and locally, S_5 is a crenulation of S_3. All of these foliations are overgrown by 1-5 cm cordierite porphyroblasts associated with the late stage, low pressure metamorphism (in outcrops before curve in river). Also observed within Sandy Creek are extensional crenulation cleavages crosscutting the regional foliation at a high angle. These cleavages contain discontinuous segregations of biotite. The cleavages strike west-northwest and dip either northeast or southwest.

Rocks along Sandy Creek show evidence for both the medium P dynamothermal metamorphism and the late low-P, amphibolite-facies metamorphism (e.g. cordierites mentioned above). Metamorphic mineral growth occurred during the formation of all foliations. Alignment of micas and amphiboles and segregations of metamorphically differentiated minerals define all fabrics. Carlson and Nelis (1986) documented staurolite preserved as inclusions in garnet in local pelitic rocks from this locality. The garnet containing the inclusions overgrows early foliations (S2, S3) but not later foliations (S4, S5), indicating that it and the staurolite grew during syndeformational metamorphism.

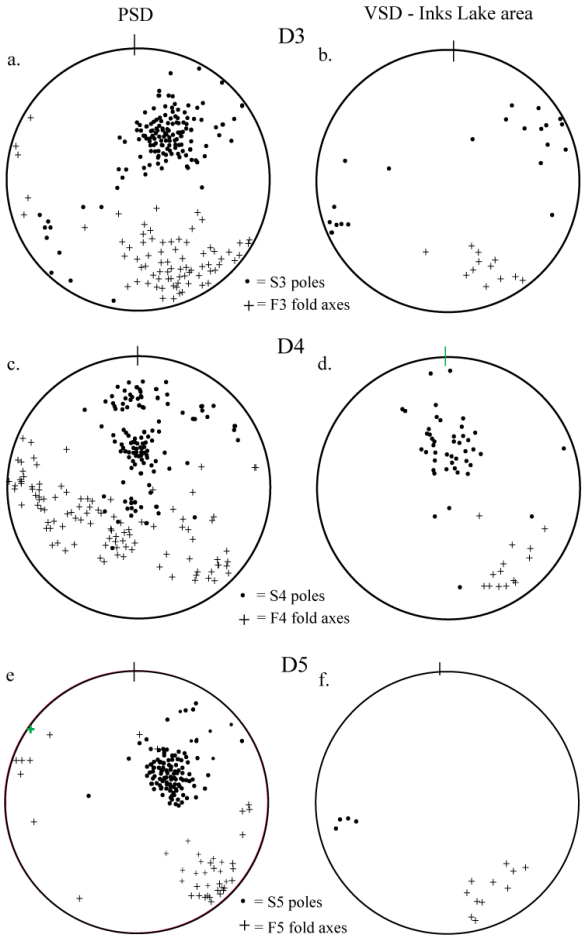

Figure 9. Orientations of structural elements D3-D5 in eastern uplift for Packsaddle domain (A, C, E) and Valley Spring domain (B, D, F).

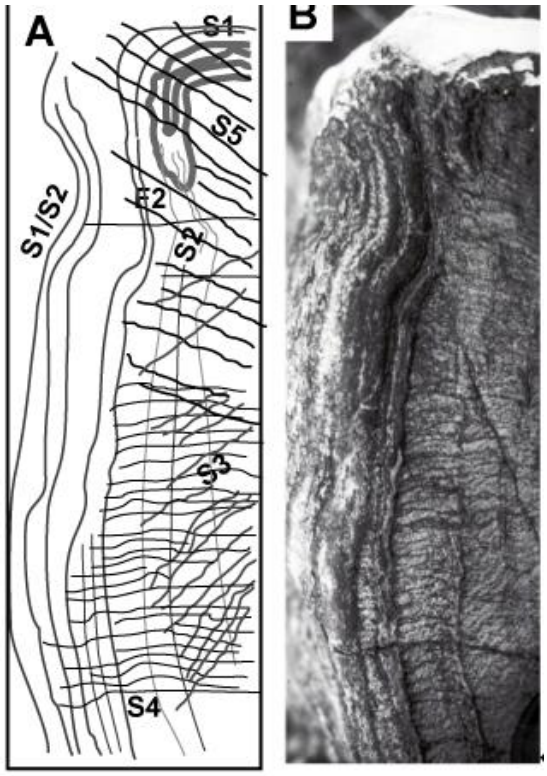

Figure 10. Limb of F5 fold showing cross cutting relationships of five foliations. All but S1 are crenulation cleavages with biotite differentiation. Sketch at right shows relative age of foliations. (From Reese and Mosher, 2004).

About 2 km to the north along the river, the 1238 +8/-6 Ma, Red Mountain Gneiss forms a large granitic sill with smaller, thinner sills intruded into the country rock at the lateral ends. These sills are isoclinally folded by F_2 folds and contain a penetrative axial planar S_2 foliation.

Drive from ford at Sandy Creek 4 miles along gravel road to low water crossing at White Creek. The outcrops are on the west side of the creek. Although this is an optional stop, a longer description has been included because it is relatively easy to get permission to stop at this location. **[Note, however, permission must be obtained to visit this locality.]**

Optional **STOP 3:** **White Creek Ford**, Packsaddle Schist domain.
The following description is modified from Reese (1995; 1996 in Mosher, 1996) and Mosher and Reese (2004)

Dominant rock types in this part of Packsaddle domain are micaceous and amphibolitic schist, quartzofeldspathic gneiss and schist, amphibole-epidote gneiss, leptite, amphibolite, and highly localized quartzite, andalusite- and staurolite-bearing

pelitic schist (Carlson and Reese, 1994). Interlayered felsic metavolcanic and metavolcanoclastic rocks dated by Reese et al. (2000) crop out south of the ford. About 4 km south of the ford prominent knobs of quartzite and 10 cm to 2 m thick muscovite schists, garnet-staurolite-sillimanite-biotite-muscovite schist, and microcline-andalusite-muscovite schist crop out. Several of these units indicate intense surficial chemical weathering prior to ductile deformation (Carlson and Reese, 1994). This part of the Packsaddle Schist is considered to be predominantly a metasedimentary, supracrustal, basinal succession of rocks (Reese, 1995), with interlayered felsic and mafic igneous components (McGehee, 1979) of probable island-arc derivation (Garrison, 1981a & b).

Rocks exposed at the White Creek ford include felsic and micaceous schists, leptites, and chloritic and amphibolitic schists. These rocks underwent multiple phases of ductile contractional and extensional deformation and metamorphism related to Grenville orogenesis. At the ford, structural elements that are exhibited include: (a) recumbent, isoclinal folds (F_2), and associated axial planar foliation (S2) and intersection lineation (L2), (b) NE-verging, chevron folds (F3), and associated axial planar differentiated crenulation cleavage (S3), both which refold D2 structures, (c) SE-plunging, open folds (F5?), and (d) a suite of post-D3 extensional structures. Crosscutting the multiply deformed metamorphosed sequence a few 10's of meters south of the main exposure at the ford is an E-W-trending, undeformed, unmetamorphosed melarhyolite dike. The dike is dated at 1098+3/-2 Ma (U-Pb zircon; Walker, 1992) and places an upper constraint on the timing of deformation in this part of the uplift.

D2 structures are especially conspicuous within thin compositionally layered schistose units like those exposed at the ford. F2 isoclinal folds are similar and recumbent, with northwest-striking axial planes and axes that plunge shallowly to the south-southeast. A well-developed S2 metamorphic layering formed parallel to the axial planes of F2 isoclinal folds. S2 is commonly parallel to S0/S1 compositional layering except in F2 fold hinges, where S2 crosscuts S0/S1. S2 is less penetrative and intense through these hinges. A prominent L2 lineation is commonly present in well-layered units and typically plunges shallowly to the south-southeast and is parallel to F2 fold axes. The S2 metamorphic layering at the ford is folded by at least two generations of folds. F3 folds are most prominent and refold the S2 foliation and locally refold F2 isoclinal folds. F3 folds are tight, NE-verging, chevron to semi-chevron folds and are developed in all rock types. S3 is axial planar to F3 folds and is typically a crenulation cleavage with biotite differentiation along foliation planes. F3 fold axes plunge gently south-southeastward (S30°E) with axial planes and associated cleavage striking northwestward and dipping gently to moderately southwestward. Locally and particularly west of White Creek, F3 folds are refolded by small, open, round to chevron, SE-plunging, nearly upright folds correlative with F5 folds in Sandy Creek.

Well displayed at the ford are a suite of related post-D3 and possibly later, extensional structures including extensional crenulation cleavages, boudinaged quartz veins, and quartz vein fibers all suggest post-D3 extension. All of these structures formed relatively late in the ductile deformational history, but prior to granite plutonism and static reheating, and indicate NNE-oriented extension. A distinctive structure at the White Creek ford ("tiger stripes") is a biotite differentiation extensional crenulation cleavage. The cleavage is nearly everywhere defined by the differentiation of biotite into discrete though discontinuous bands. In many occurrences, normal offset of folia, especially S2, is indicated across crenulation cleavage planes. The crenulation cleavage strikes west-northwest and dips variably both to the northeast and southwest. This cleavage is associated with two sets of quartz veins that crosscut F_3 and S_3. The most prevalent veins strike northwest and systematically dip 25^o-35^o more steeply to the southwest than S_2/S_3. Quartz vein surfaces preserve aligned fibers plunging shallowly to the south or south-southeast (similar to slickenfibers), indicating a component of vein-parallel shear during formation. In places, the fibers have been pulled apart and filled with non-fibrous quartz in zones nearly perpendicular to the fibers, suggesting either a change in strain rate during formation or later extension of the veins parallel to the fibers. These quartz-filled, pull-apart zones are nearly parallel to the strike of the extensional crenulation cleavages in the same outcrop. Rarely, veins in this orientation form nearly en echelon arrays parallel to S_2/S_3, suggesting the possibility of local top-to-the-south shear. Some of these veins are boudinaged with boudin neck axes oriented west-northwest. Quartz fibers oriented nearly orthogonal to the boudin necks affect the margins of the veins and are best expressed in the neck regions, indicating that their formation is related to the extension. Minor west- striking, steeply dipping, quartz veins are gently folded with north-plunging axes. Taken together, the combined geometry of these extensional structures favors north-northeast-oriented extension and vertical shortening, with a possible minor component of northwest-trending, left-lateral strike-slip motion.

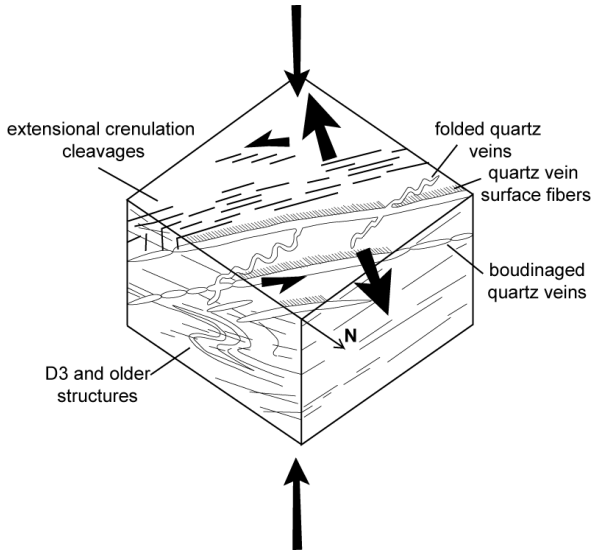

Figure 11. Schematic diagram showing geometric relationships of extensional structural elements in White Creek area. (From Mosher and Reese, 2004).

Rocks along White Creek show evidence for both the medium P dynamothermal metamorphism and the late low-P, amphibolite-facies metamorphism. Similar to Sandy Creek, metamorphic mineral growth occurred during the formation of all foliations. Alignment of micas and amphiboles and segregations of metamorphically differentiated minerals define all fabrics. Along White Creek, approximately 4 km south of the ford, Fe-rich staurolite in rare pelitic assemblages is elongate and preferentially aligned with the

dominant foliation in the rock (S2). The staurolite overgrows relict fold hinges of elongate quartz inclusions, which most likely represents S1 folded by F2, indicating that it is mimetic to a syn-S2 mineral but still grew early during deformation. The reaction of staurolite + quartz = garnet + sillimanite is exhibited in this unit, suggesting that pressure-temperature conditions may have been on the order of 700°C and 7 kbar during deformation (Carlson and Reese, 1994). Evidence for later thermal metamorphism is abundant in the White Creek area, although not clearly demonstrated at the ford. Randomly oriented minerals such as andalusite, actinolite-tremolite, biotite, muscovite, and possibly sillimanite are observed (Carlson and Reese, 1994) that overprint deformation textures indicates that static recrystallization occurred at high temperatures and low pressures.

After ford at White Creek continue 0.9 miles to the intersection of CR 310 with Highway 71. Take a left onto Highway 71. Turn left and drive west 6.3 miles to crossing with Honey Creek. Park in large roadside park on the right just before the crossing. Walk along highway to outcrop watching for cars.

STOP 4: **Highway 71 outcrop**, just west of Honey Creek, near northern boundary of Packsaddle domain with the Valley Spring domain.
The following description is modified from Mosher, 1996.

This outcrop of black, graphitic phyllite with interlayers of light-brown, quartz-rich phyllite and minor biotite schist shows a well developed foliation that is axial planar to abundant isoclinal folds (F_2). Folds are best displayed where the light brown, quartz-rich phyllites are interlayered with the graphitic schist. [For example, near the roadbed just west of the white reflector pole.] A mineral lineation (L_2) is parallel to the SE-plunging fold axes. The foliation in this area strikes northwest and generally has moderate dips. This foliation is the dominant foliation (S_2) found throughout the uplift. Thin quartz veins locally cross cut or parallel the foliation and are both folded and boudinaged. The foliation is also locally folded by late, open folds.

Figure 12. F2 fold in graphitic schist; note axial planar S2.

The phyllites are intruded by small granitic pegmatites that locally distort the foliation. The graphitic phyllite shows a beached zone around the intrusions, indicating volatilization of the graphite during intrusion.

North along Honey Creek just west of this outcrop, these phyllites are interfolded with marbles, calc silicates, and amphibolitic schists in large-scale, isoclinal F_2 folds. These F_2 folds and the S_2 foliation are folded about regional- to outcrop-scale, E-trending, F_4 chevron folds and broad open F_5 folds. About 5 km north of the highway, Packsaddle domain rocks are thrust northeastward over the Valley Spring granitic gneisses along a ductile shear zone (Fig. 5). The upper Valley Spring domain exposed here represents a highly attenuated intrusive igneous complex (Zumbro, 1999). Just above

the contact a metavolcanic unit in the Packsaddle domain yielded a U/Pb zircon crystallization age of 1247+/-4, whereas augen gneiss in the uppermost part of the Valley Spring domain yields a crystallization age of 1272 +8/-5 Ma (Reese et al., 2000). These two units lie within the mylonite zone at the boundary of the two domains. Rocks from this area, but slightly lower within the Valley Spring domain, yield an 1366+/-3 Ma crystallization age and a 1325+/-5 Ma metamorphic ages (Honey Creek gneiss of Reese et al., 2000), interpreted to represent Laurentian basement. **[*Unfortunately, access to this creek is highly restricted*.]**

Continue NW on Hwy 71 for another 5.8 miles. Turn right and follow CR 306 for a short distance. Park at the Hussey Ranch, on the right side of the road.

Stop 5. Hussey Ranch, Valley Spring domain with relict eclogites
The following description is modified from Zumbro, 1999; Mosher et al., 2004; Carlson et al., 2007).

This stop lies within the Valley Spring domain and shows the relationships between felsic gneisses and garnet clinopyroxenites that are relict eclogitic bodies. Here two large tear-drop shaped bodies of retrogressed eclogite, ~ 5 m in diameter, and several smaller nodules are found within well foliated felsic gneisses. These nearly spherical bodies are wrapped by the surrounding gneisses and foliation. On the basis of field relations at the nearby Edwards Ranch (discussed below), Zumbro (1999) and Mosher et al. (2004) interpret these bodies as isolated boudins. We will examine one of these larger bodies, which is bounded on one side by a foliated aplitic layer. This layer separates the body from thin mafic layers of apparently the same composition.

Figure 13. Spherical boudin of relict eclogite wrapped by S2, felsic gneisses and foliated aplite.

The eclogitic bodies, themselves, are retrogressed to amphibolite at their margins and have a moderately well-developed foliation that parallels the margins (Zumbro, 1999l Carlson et al., 2007). This foliation is continuous with the S_2 foliation in the surrounding rock. The recrystallized assemblage is hornblende+ oligoclase ± augite. This foliation and amphibolitization dies out gradually toward the unfoliated centers of the bodies. Garnet is relatively well preserved in the cores of bodies, but was progressively resorbed outward toward their foliated margins. All portions of the bodies show coronas around garnet and symplectitic replacement of original sodian clinopyroxene identical to the strongly retrogressed portions of otherwise well-preserved eclogites found in the western uplift. No primary sodic clinopyroxene in the matrix surrounding garnet porphyroblasts remains.

The interior portions of the eclogite bodies contain a compositional layering (centimeter to decimeter scale) defined by differences in the abundance of garnet relative to other phases (Zumbro, 1999; Carlson et al., 2007). This internal layering is at a high angle to the foliation at the margins. This layering is interpreted to result either from original compositional differences in an igneous precursor, or possibly from metamorphic differentiation during eclogite formation.

Inclusion suites in garnet show a transition from core to rim (Carlson et al., 2007; Mosher et al, 2008). In garnet interiors, inclusions record an amphibolite-facies assemblage: quartz, andesine, epidote/clinozoisite, tschermakitic amphibole, and ilmenite. The rims lack plagioclase and ilmenite, and instead contain rutile. Epidote and amphibole inclusions in rims are rarer than in interiors, and amphibole in rims tends to be pargasitic. This distinct change in the inclusion assemblage is interpreted to represent initial garnet growth in an amphibolite-facies matrix, but final crystallization in an eclogite-facies matrix. Peak pressures are a minimum of 1.4 GPa using GRIPS barometry. At the nearby Edwards Ranch the same pressures are found, and temperatures are 643 ± 10 using Fe-Mg exchange between garnet and amphibole (calibration of Graham and Powell; 1984 with all Fe as Fe2+). Garnets retain steep growth zoning profiles, indicating peak temperatures insufficient for homogenization by intracrystalline diffusion.

Nearby at Edwards Ranch, cliff faces along a creek show boudinage of once-continuous layers that were apparently conformable to the compositional layering in the surrounding felsic gneiss (Zumbro, 1999; Carlson et al., 2007; Mosher et al., 2008). The numerous elliptical to near-spherical boudins of relict eclogite, decimeters to meters in diameter, are retrogressed to amphibolite within the boudin neck regions as well as along their margins. Many boudins are connected by thin amphibolite layers and other thin layers appear to be completely retrogressed ecolgitic bodies. Boudinage of eclogite layers started early in the deformational history as shown by the strong competency contract resulting in the nearly spherical boudins. Additional boudinage took place under amphibolite-facies conditions, apparently during continued deformation following creation of the dominant S2 foliation in the gneisses wrapping the boudins (Zumbro, 1999; Mosher et al., 2004).

Return to Hw 71 and turn left. Drive to CR 307 and turn left (north) towards Kingsland. At intersection with Rt. 1433 turn left and drive to intersection with HW 29. Turn righ (east) on Hwy 29. Approximately 1 mile after crossing the Colorado River, turn south onto Park Road 4. Follow the road to Inks Lake State Park; turn right into the park headquarters entrance. Once in the park, follow the road north as it winds through the campground to the northernmost camping loop (sites 241-257) and park opposite the playground. From here it is a short walk to the Devils Waterhole at the mouth of Spring Creek.

<u>Stop 6:</u> Inks Lake State Park, Devil's Waterhole, Valley Spring domain at Spring Creek. *The following description is modified from Hoh (2000), Mosher et al. (2004) and Hoh (2004).*

This stop consists of polydeformed, quartzofeldpathic gneisses, migmatites,

amphibole gneiss, pelitic schists and gneisses and a granitic sill, all metamorphosed at uppermost amphibolite facies and intruded by late granites. Much of the rest of the Valley Spring exposed in the area is a ubiquitous pink, biotite gneiss with a crystallization age of 1232 ± 4 Ma (Walker, 1992; Inks Lake gneiss of Reese et al., 2000). Detailed structural mapping by Hoh (2000) identified five foliations and four associated generations of folds. Four of the foliations (S1/S2, S3, and S4) are penetrative throughout the field area. S5 is found only locally in the hinges of the large F5 folds. We will begin at the top of the hill where the large scale structures and relationships are well exposed in the exposures across the creek, and then proceed down to the creek and to the east to look at structural relationships.

Figure 14. Overview of intrusive relations at Devil's Waterhole, Inks Lake State Park.

Spring Creek exposes a large-scale F5 antiform that folds lithologic layering and the composite S1/S2 regional foliation. A foliated and polydeformed sill dated at 1253+3/-2 Ma is observed in the opposite hillside and is repeated across this antiform. It will be seen again at the end of our traverse at the waterfall. The polydeformed units are intruded by undeformed to weakly deformed crosscutting granite dikes. These granites are most likely related to the Town Mountain suite of granites, represented by the nearby Kingsland pluton. Dikes that crosscut F5 axial planes are undeformed, but those parallel to the F5 axial planes are slightly boudinaged and contain a fabric in the boudin necks.

The geometries, orientations and superposed relationships of the structures are similar to those in the Packsaddle domain (Fig. 9), however, at least three generations of leucosomes are observed parallel to the first three foliations. Many of the features can be readily observed along the creek.

- S1 can only be distinguished from dominant S2 fabric in the hinges of F2 folds. Where identified, S1 is defined by the alignment of micas or amphiboles and parallel leucosomes. The leucosomes (this and all other generations) are composed primarily of microcline ± plagioclase ± quartz ± biotite ± chlorite ± muscovite, with greater or lessor amounts of each mineral in different leucosomes. Leucosomes tend to be microcline dominant even when the host rock has more plagioclase than microcline.
- S2 is defined by a metamorphic segregation of biotites, amphiboles, and opaques versus quartz and feldspar, aligned biotite, and a parallel generation of leucosomes. S2 is axial planar to rarely observed isoclinal F2 folds that plunge southeast.
- The most commonly observed fold generation at this stop is F3 (Fig. 15). These folds are well exposed in the creek where they fold the pronounced S2 fabric and parallel leucosomes. In general, F3 have a slightly more open style than F2, and are less wispy in appearance. The mean plunge of the F3 folds is S23°E/30° with northwest striking, steeply south-dipping axial planes. F3s fold leucosomes, S1, and S2 and are cut by S4 and S5. S3 is a penetrative, but generally poorly developed foliation in the field. It is roughly parallel to S1/S2 in much of the field area, but can be easily distinguished in the hinges of F3 folds, where aligned biotite parallel to S3 cut across

the folded S1/S2 fabric and parallel leucosomes. S3 is defined by aligned biotite, muscovite, and sillimanite (in pelitic rocks), and leucosomes.

Figure 15. S2 and parallel leucosomes folded by F3 folds; F3s folded by F4. Note S4 axial planar to F4.

- F4 folds are open folds that trend S35°E/30° and have east striking, north dipping axial planes. F4 folds are most easily recognized folding F3 axial surfaces, where F4 folds strike at a high angle to the F3 folds. The overprinted structure results in an isoclinal fold with a gently curved axial trace. An excellent example is at the end of our traverse near the waterfall (Fig. 15). S4 is a penetrative foliation that cross cuts and strikes at a high angle to the earlier foliations in the field. S4 is defined by aligned biotites or amphiboles (but no leucosomes) and is better developed on the eastern end of the field area. S4 strikes east-west and dips shallowly to the south.
- F5 folds are open to tight folds that plunge S23°E/30° and vary from upright to overturned to the southwest through the field area. The large antiform that repeats the units across the field area is an F5. The scale of these folds ranges from being on the order of 100's of meters to ~0.5 meters. Several small parasitic F5 folds are observable along our traverse. The hinges of F5 folds contain a crenulation cleavage and a series of parasitic folds that, along with their more open nature, makes F5 folds distinct from F3 folds. S5 is recognized locally in a couple of F5 fold hinges, mainly in the western portion of the field area. S5 is defined by an alignment of micas and amphiboles, and can be quite penetrative, where present. S5 strikes north-northwest, and dips steeply to the east. No leucosomes are parallel to S5 or are recognized accompanying F5/S5.
- Boudinage is common throughout the study area. Small-scale (< 3 cm) boudinage is seen mainly in the leucosomes parallel to the various S-surfaces, which may be related to fabric formation. Larger-scale boudins (~0.5m), which show extension to

the northwest, are parallel to and affect the S1/S2 foliations and F3 folds. The necks of these boudins are filled with quartz, suggesting that melt was not present to fill in the interstices during their formation (post-F3). A good example is about half way along the traverse.

- F1/S1 through F3/S3 occurred at uppermost amphibolite facies conditions. Peak conditions occurred during F2/S2 and are constrained to temperatures over 700°C and to pressures less than 10 kbar. After F3/S3, sillimanite is replaced by muscovite, and no leucosomes are generated, suggesting that metamorphic conditions drop into amphibolite facies and remain there through the formation of F5/S5.

At the eastern end of our traverse by the waterfall, the superposed relationships between F2/S2, F3/S3 and F4/S4 are well displayed in the migmatites. The foliated and polydeformed sill crops out on the eastern limb of the large F5 antiform. This foliated sill dated at 1253 +3/-2 Ma is apparently intrusive into the surrounding mafic gneiss; the latter yields a metamorphic age of 1129±4 Ma. Adjacent to these units is a pelitic schist containing sillimanite.

Retrace your path back to the parking lot. Exit the park along the same route. Turn left onto Park Road 4 and retrace the route back to Rt. 29. Turn left (west) follow Rt. 29 to Llano.

Day 2

We will begin the day looking at several exposures of the Valley Spring and Packsaddle domains in the western uplift to compare lithologic, structural, metamorphic and age relationships with those in the eastern uplift. ***Permission to visit these stops must be obtained from the landowners.*** We will end the day making several stops where we will examine the late stage granites and their relationships to the structures while traveling towards Austin. See Figures 2 and 16 for locations.

From the Lone Star Inn in Llano head west on combined Highways 29 and 71. After 2.2 miles 71 and 29 split and we will stay on Hwy 29. We will continue past the turnoff to Castell, on CR 2768 and past the Mason County line. At 20.8 miles, turn left (south) onto Bauerville Road. Drive for 2.4 miles along Bauerville Road toward the Llano River. At mile 2.4 take a right onto an unmarked road that leads to the Eudaly cabin. Park at the cabin and walk down to the river.

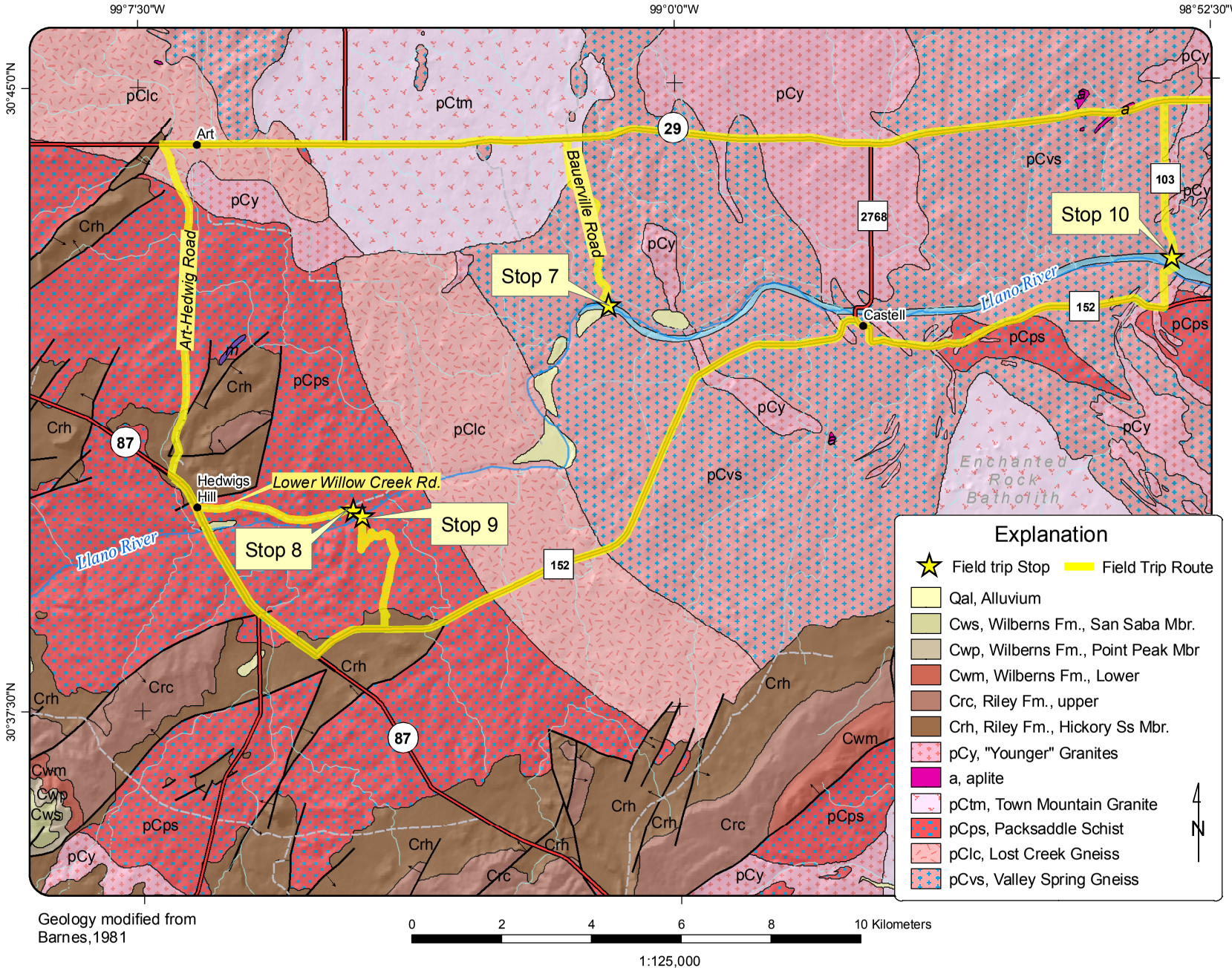

Figure 16. Geologic map of the southeastern Llano uplift, showing Stops 7-10.

Stop 7. Eudaly Ranch; Valley Spring domain, western uplift

N.B. This outcrop is on private property. Permission to visit must be obtained from the landowner. *The following description is modified by J.S. Levine from Levine (2005).*

The Valley Spring domain in the western Llano Uplift is comprised of both para- and orthogneisses with abundant migmatites found within both rock types. Five phases of deformation (D_1-D_5), each defined by ductile folds (F_1-F_5) and axial planar foliations (S_1-S_5), occur on a microscopic to regional scale and were accompanied by dynamothermal metamorphism at uppermost amphibolites-facies conditions. The first three phases of deformation, D_1-D_3, are characterized by structures and metamorphic textures that indicate temperatures at or above the solidus. In pelitic rocks, sillimanite parallels S1-S3. The later phases of deformation, D_4 and D_5, also took place under amphibolites-facies conditions, but the structures and fabrics do not provide evidence for higher T conditions. Syn- to post-tectonic granites and pegmatites are abundant throughout the field area and may be associated with an extensional D_6 phase of deformation.

The S_1 foliation is a well-developed metamorphic layering axial planar to F_1 isoclinal folds and generally sub-parallel to compositional layering, S_0. S_1 is difficult to distinguish from S_2 in the field because F_2 and F_3 folds have folded into parallelism with S_2. F_2 folds are generally isoclinal with a penetrative axial planar foliation, S_2. The S_1 and S_2 foliations form a composite, well-defined foliation, which is the dominant foliation seen in the uplift. Leucosomes commonly parallel both foliations. The composite S_1/S_2 foliation strikes dominantly to the northwest and dips to the east, although its orientation is affected by later refolding. F_2 fold axes plunge shallowly to the east-southeast.

F_3 folds are tight folds of the well-defined S_1/S_2 composite foliation with an axial planar foliation, S_3, at approximately a 30° angle to S_1/S_2 foliation. Early structures are refolded by F_3 folds and commonly form interference patterns such as eyes. The S_3 foliation is a well-developed metamorphic foliation with leucosomes generally parallel to it, but it is not as penetratively developed as S_1/S_2. A few outcrops in the field area show evidence of progressive folding during D_3. Two sets of folds, F_{3A} and F_{3B}, can be identified by the structures they fold. F_{3A} folds F_2 folds and S_2 foliation and are folded by F_{3B} folds. F_{3B} folds F_{3A} and are folded by F_4 folds. F_3 folds plunge to the east-southeast at a moderate to shallow angle; the foliations strike northwest and dip to the northeast.

Two later generations of open folds, F_4 and F_5, fold all earlier structures and are seen on an outcrop to regional scale. F_4 and F_5 locally have associated axial planar foliations, S_4 and S_5, which are defined by aligned metamorphic minerals, but were definitively identified only in thin section. F_4 folds trend northeasterly and their fold axes plunge to the east-northeast. F_5 folds trend to the northwest and their fold axes plunge to the southeast.

Throughout the Valley Spring Gneiss there are abundant granitic and pegmatitic veins and dikes, which cut across and are folded by various generations of folds. Many pegmatites are folded by F_2 and F_3. In addition, boudinage and shearing locally affect early structures and pegmatites; both of these structures are likely associated with D_6

extension. Larger granitic plutons, more widespread than the smaller granitic and pegmatitic veins, cross cut all structures and are undeformed. These post-tectonic granites have xenoliths containing the S_2 foliation.

This stop shows crystallized melt parallel to S_1, S_2 and S_3 foliations. F_2 folds of S_1 foliation and parallel quartz/feldspar rich layers that appear to have been the result of partial melting are abundant. An axial planar foliation, S_2, also contains thin segregations of quartz/feldspar that either formed in situ or was injected parallel to the foliation. The S_2 foliation and F_2 fold were later refolded by F_3 folds (Fig. 17). There are additionally thick quartz/feldspar segregations that are sub-parallel to the S_3 foliation. The thin quartz/feldspar segregations parallel to S_1 and S_2 either formed in situ or were injected, while the thicker segregations parallel to S_3 appear to have formed in situ (Fig. 17). Thus melt was definitely present during D_3 and may also have been present during D_1 and D_2.

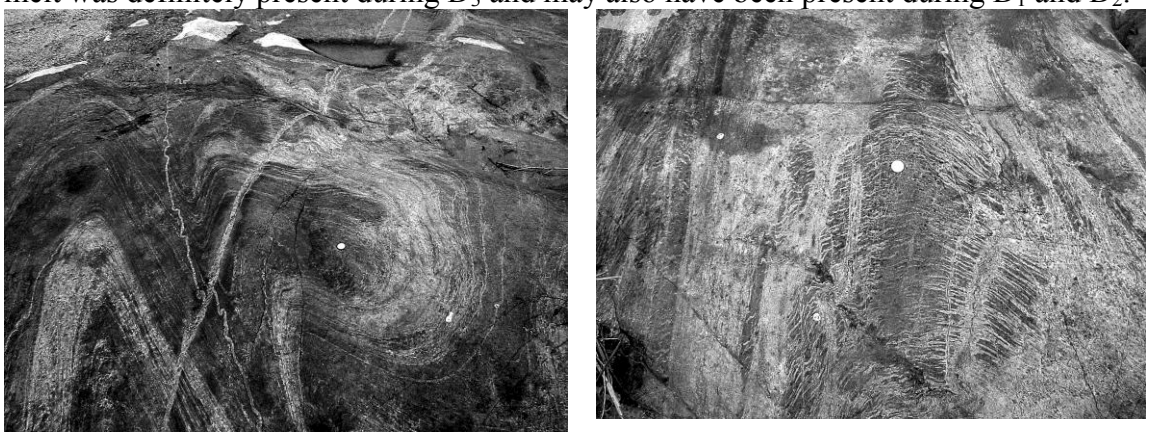

Figure 17. F2 folds of S1 and parallel leucosomes are folded by F3 folds (left); relationship between diffuse leucosomes parallel to S3 and thin segregations of quartzofeldspathic material parallel to S2 (right).

Pegmatites are also present in this locality and both pre- and post-date F_2 and F_3 folds. There is a ptygmatically folded pegmatite vein that contains F_2 folds that have been refolded by F_3 folds, leading to complex interference patterns between the two generations of folding. Additionally, there are pegmatite veins that cross-cut the large F_3 folds that have folded the quartz/feldspar segregations parallel to S_2. This illustrates the presence of pegmatites throughout deformation, with some deformed during the earlier hotter phase of metamorphism and others intruding later in the deformation as the temperature decreased.

Upon return to the vehicles, drive back to the Bauerville Road. Turn left and drive 2.4 miles back to the intersection of the Bauerville Road with Hwy 29. Take a left onto Hwy 29. Drive 5.6 miles and take a left on Art-Hedwig Road. This road is about 0.4 miles past Lower Willow Creek Road. Take the Art-Hedwig Road until it intersects Hwy 87. Take a left on Hwy 87 (divided highway) and within 0.2 miles you will see a sign for Lower Willow Creek Road. Take a left here and follow this road for about 2.2 miles. Take a right into the Hunt property.

Stop 8 Worrell property, Lower Willow Creek Road, Mason County. Packsaddle domain, western uplift.
N.B. This outcrop is on private property. Permission to visit must be obtained from the landowner. *The following description is by M. A. Helper; also see Roback et al. (1999) and Hunt (2000).*

Much of the magmatic and polydeformational history of the western Llano uplift is contained in this small (~100 m^2), water- polished outcrop of Packsaddle Schist. Polydeformed, interlayered mafic and felsic orthogneiss contain dikes and sills of three distinct ages (Fig. 18) that provide both relative and absolute age brackets for five phases of folding and metamorphic fabric development. The outcrop and the history it contains were initially described by Hunt, Helper, and Roback (1996) and then analyzed in detail by Roback, Hunt and Helper (1999). Subsequently, Hunt (2000) extended his detailed structural mapping into the surrounding region, discovering aspects of the deformational, metamorphic and magmatic history not recorded here. Consequent revisions to fold, fabric and magmatic phase nomenclature (e.g. F2, S3, I4, etc.) at this outcrop resulted, as did a reinterpretation of the constraints on the age of the earliest dynamothermal event (D1). These revisions, fully described by Hunt (2000), are incorporated in the figures and descriptions below.

Lithologies present in this outcrop are:

1) Felsic Gneiss**:** light gray, fine- to medium-grained quartz-plagioclase-biotite banded gneiss with compositional layering (S0) defined by varying amounts of biotite. Aligned biotite defines a foliation (S1/S2) that is parallel to compositional layering. Conformable discontinuous veins and pods of quartz are ubiquitous, but most common in fold hinges. Contacts with mafic gneiss are sharp to gradational. Prismatic euhedral to subhedral zircon morphologies are consistent with an igneous origin for this rock type but do not yield a precise crystallization age. Metamorphic zircons (low U and model Th concentrations, stubby grains) in this lithology (locality A, Fig. 18) are, however, concordant, giving a date of 1256$\pm$4 Ma (Roback et al., 1999). Titanites in the same sample record a U/Pb age of 1114 $\pm$ 3 Ma, and metamorphic rims on zircons from felsic gneiss about 400 meters east of this outcrop yield an age of 1123.8 $\pm$ 8.5 Ma (A. Pettersson and D. Cornell, unpublished SIMS data). These younger dates are consistent with U/Pb ages for D1-D5 dynamothermal metamorphism and cooling (and/or resetting) elsewhere in the uplift (Roback et al., 1999; Mosher et al., 2008). The 1256 Ma metamorphic date is, within error, coeval with crystallization ages for the oldest dated sills in this outcrop, a metaplutonic body nearby (Lost Creek Augen Gneiss) and other meta-igneous rocks of the eastern uplift, suggesting this earliest metamorphism accompanied a period of widespread magmatism (Hunt, 2000).

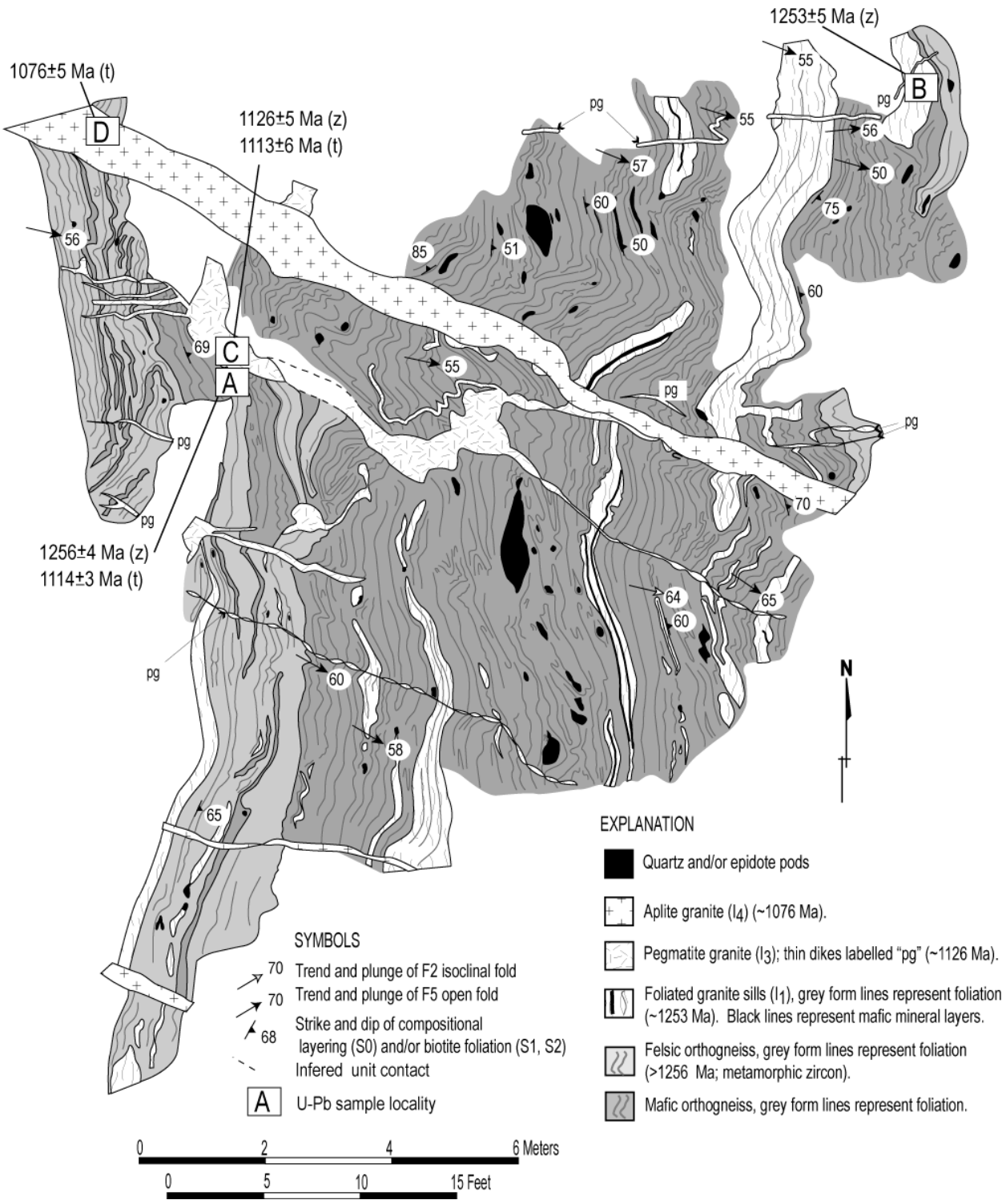

Figure 18. Geologic map of the outcrop at Stop 8, modified from Hunt et al. (1996). The outcrop is surrounded by recent alluvial deposits, shown in white. U/Pb ages (z-zircon, t-titanite) are from Roback et al. (1999), which also contains a color version of this figure.

2) Mafic Gneiss**:** black to dark gray, fine- to medium grained hornblende-biotite-plagioclase±quartz±potassium feldspar banded and lineated gneiss. Compositional banding (S0) is defined by mm- to cm-thick layers with varying proportions of mafic and felsic minerals. Thin (<1.0 cm) felsic mineral-rich layers are compositionally identical to thicker layers of felsic gneiss described above. Mafic gneiss contains conformable but discontinuous pods (< 0.5m) and mm- to cm-scale stringers of epidote (locally rimmed by hornblende) and discontinuous veins and pods of milky quartz. Three foliations (S1, S2 and S5) defined by aligned biotite can be observed in thin section. Compositional layering (S0) is parallel to S1 and, except in F2 fold hinges, subparallel to S2. S5 (see below) is more weakly developed and perpendicular to the other two. Hornblende and biotite define a lineation (L2) on foliation surfaces.

3) Foliated Granite: gray to light pink, discontinuous lenses and layers of fine grained, foliated granite. Larger bodies are compositionally layered (S1), containing biotite and quartz-feldspar layers that are folded (F2). A foliation (S2) defined by biotite and flattened quartz and feldspar is axial planar to these folds. Quartz-feldspar layers are locally strongly lineated, containing coarse (up to 1 cm) quartz and feldspar rods (L2) that are collinear with F2 fold axes. Fabrics within these granites are collinear and coplanar to those in the surrounding gneiss, demonstrating that intrusion predated the earliest fabric forming events (D1 and D2). Magmatic zircon in this lithology (locality B, Fig. 18) gives a U/Pb crystallization age of 1253 +5/-3 Ma (Roback et al., 1999). These are the earliest granitoid sills (I_1) yet identified in the western uplift.

4) Pegmatitic Granite: coarse-grained to pegmatitic, containing pink microcline and accessory biotite. Primary igneous textures and mineralogy are preserved. Present as folded or boudinaged, cm- to decimeter-scale dikes and veins that transect compositional layering and foliation in the gneisses and foliated granite (Fig. 18). In the relative chronology developed from regional mapping, this is a 3rd generation granite (I_3) that was intruded after D1-D3 transposition and folding, but before D4-D5 folding. On the basis of orientation and relative age, boudinage and folding of I_3 granite here is consistent with deformation during D5 (F3 and F4 folds are not present in this outcrop). Pegmatitic granite in this outcrop (locality C, Fig. 18) has a U/Pb zircon crystallization age of 1126 ± 5/-4 Ma and gives a Pb/U titanite cooling age of 1113 ± 6 Ma (Roback et al., 1999).

5) Aplitic Granite: undeformed, pale pink to gray, fine grained, containing pink microcline and accessory biotite. Centimeter- to decimeter-scale northwest trending veins and dikes of this granite cut all other rock types and fabrics. Primary igneous textures are visible in thin section. A weak biotite fabric parallel to dike margins is interpreted as a flow foliation. A regional suite of intrusive granite of this relative age, the I_4 intrusions of Hunt (2000), are the youngest intrusives thus far recognized in the western Uplift. Aplite granite at this outcrop (locality D, Fig. 18) has been dated at 1076 ± 5 Ma (Roback et al., 1999).

Metamorphic fabrics and structures that can be observed here are:

1) Primary (S0) compositional layering - the earliest fabric (S0) is the compositional layering between mafic and felsic gneiss, and thicker mafic and felsic layers in each of the gneiss units. This is regarded as primary in origin, though strongly transposed and enhanced during amphibolite to granulite facies dynamothermal metamorphism.

2) S1 and S2 foliations, F2 folds – the (S0) compositional layering is parallel to a biotite and/or hornblende foliation (S1) that is folded by tight to isoclinal, reclined folds (F2). A second foliation (S2), defined by biotite and/or flattened quartz and feldspar grains, is axial planar to these folds. S2 is most easily visible in thin section and in hinges of F2 folds. F2 folds and an L2 lineation, defined by elongate quartz and feldspar in foliated sills and by hornblende in mafic gneiss, plunge 40-50^{o} E. F2 folds of S0 and S1, the L2 lineation, and the S1-2 foliation are present in both gneiss units and the foliated granite sills, demonstrating that these earliest phases of deformation (D1, D2) must post-date intrusion of the granite sills at 1253 Ma. D1 and D2 deformation does not affect the two younger phases of granite, indicating D1-D2 deformation here ceased before 1126+5 Ma.

3) S5 foliation and F5 folds – two subsequent phases of folding (F3, F4), recognized elsewhere by orientation, coeval foliations (S3, S4), and relationships to granite dikes and veins (see Hunt, 2000), are not present here. The youngest folds in this outcrop are regionally equivalent to folds of the F5 phase. F5 folds here are upright, tight to open, and have a mean axis that plunges 59^{o} toward 102^{o} with a mean axial plane that strike 107^{o} and dip 76^{o} N (Fig. 19). An axial planar biotite foliation (S5) is locally developed, and pegmatitic granite veins and dikes that are parallel or subparallel to F5 axial planes are boudinaged (Fig. 18). F5 folds and boudins deform pegmatitic granite, but are cut by aplite granite dikes, indicating D5 deformation occurred between 1126 ± 5 and 1076 ± 5 Ma.

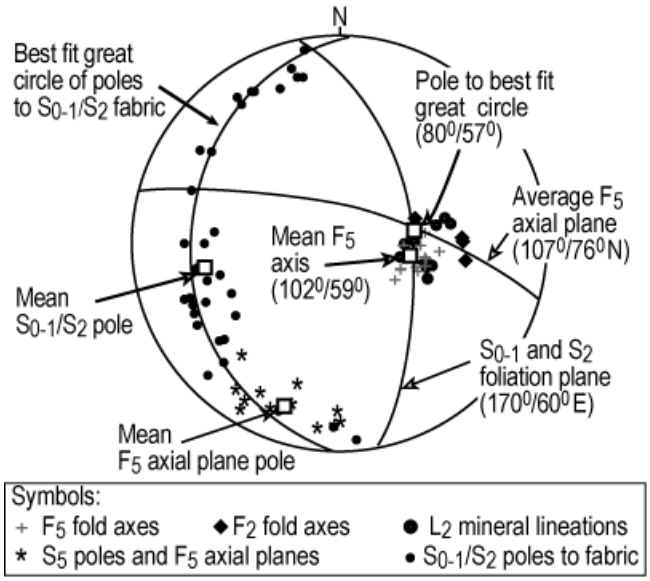

Figure 19. Equal area stereogram of fabric elements at Stop 8 (modified from Roback et al., 1999).

Exit the Hunt property and turn left. Drive 2.2 miles back to Hwy 87 and turn left. Drive 2.8 miles south on Hwy 87 over the Llano River until you see signs for a left turn onto CR 152. Turn left onto CR 152 and travel 1 mile to the Bode Ranch. Turn left and drive through the ranch to the Llano River. The outcrop is along the river to the east of the parking area.

Stop 9. Bode Ranch; Packsaddle domain, western uplift
N.B. This outcrop is on private property. Permission to visit must be obtained from the landowner. *The following description is by S. Mosher and based on Hunt (2000).*

This stop is directly across the river from the previous Stop 8 and displays similar structures and intrusive relationships. At this stop alternating felsic gneisses, well-foliated mafic layers and pegmatites are folded by open to tight F5 folds and display a spectacular set of structures (Fig. 20) described below. The S2 foliation within the layers is rarely seen to be isoclinally folded by F3 folds.

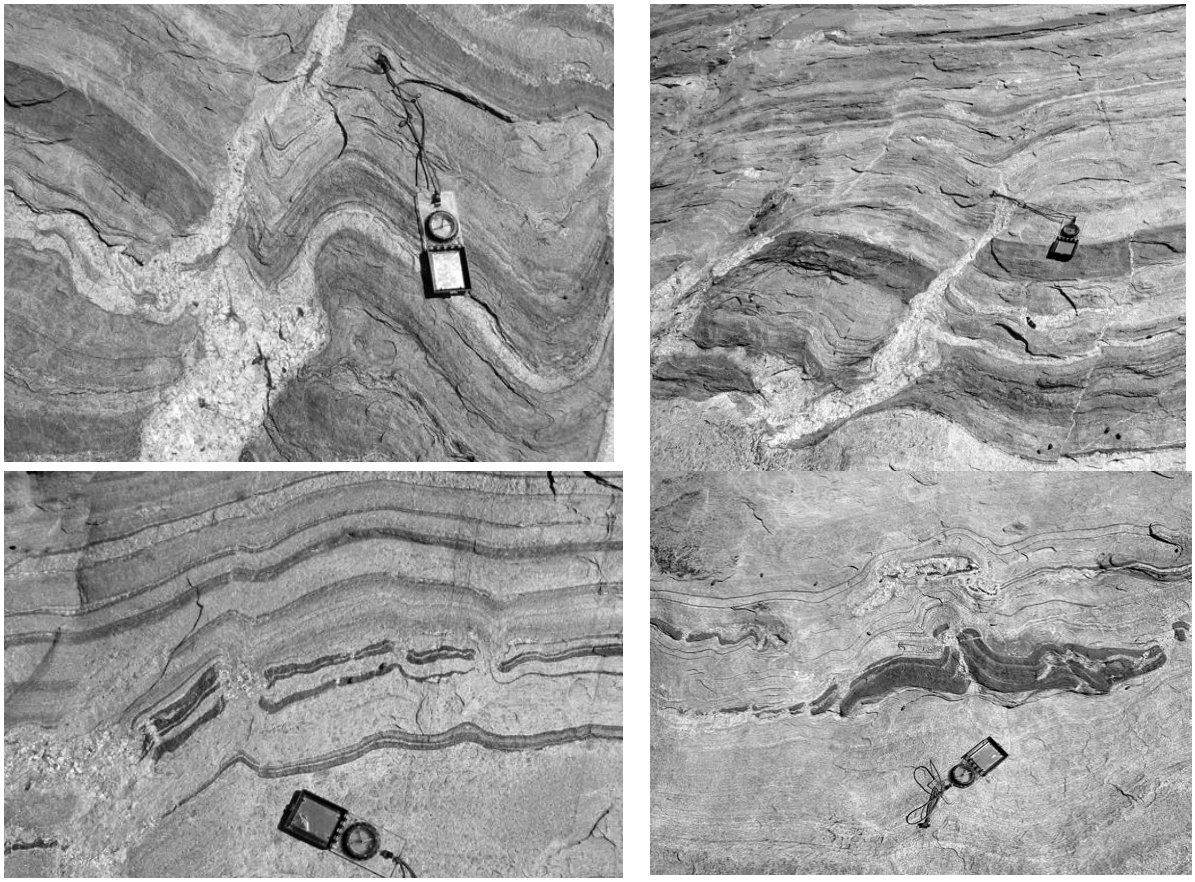

Figure 20. Relationships observed in Packsaddle at Bode Ranch. See text for description.

Mafic layers are boudinaged with felsic pegmatitic material in the boudin necks. These boudins are folded by the F5 folds. Some boudinaged layers are also bounded by pegmatitic material and fold hinges are filled with pegmatitic material. In some places, boudins have been thrust or stacked on top of each other with pegmatitic material in between. The geometries of these folded boudins and associated pegmatitic material suggests that melt was present during folding and the melt acted as "décollement" surfaces accommodating slip during shortening.

Locally layer parallel pegmatites, which are folded, are continuous with pegmatites at high angles to the layering, which form pinch and swell boudins, suggesting intrusion prior to folding. Elsewhere shorter pegmatites at a high angle to layering appear to have formed in larger boudin necks that subsequently deformed during folding. That these pegmatites at a high angle to layering formed parallel to the fold axial planes cannot be ruled out, however.

Shear zones nearly parallel to axial planes of the F5 folds are also observed with aplitic and pegmatitic material along the zones. The relationships observed at this outcrop strongly suggest that melts were present during these later stages of deformation.

Backtrack to Hwy 152 and turn left (east). Drive east on Hwy 152 along the south side of the Llano Rive to the town of Castell. Continue on Hwy 152 for 4.7 miles. Tturn left onto CR 103. Follow CR 103 0.7 miles across the Llano River and park on the north side.

Stop 10. CR 103, undeformed, late-stage, fine-grained granites
The following description is by J. S. Levine.

Fine-grained, late-stage granites intrude both Valley Spring and Packsaddle lithologies in the western Llano Uplift. Some of these younger granites are deformed, but many intruded post-deformation and contain xenoliths of deformed country rock. Some xenoliths are concordant with the structures in the surrounding rock, but many are not and have been rotated. Ages for these fine-grained granites from nearby low water crossings to the east and west of this stop, respectively, are 1113.2 +/- 1.7 Ma (Sixmile Granite; J. Connelly, unpubl. TIMS zircon data) and 1113.7 ±7.9 Ma (A. Pettersson and D. Cornell, unpubl. SIMS zircon data).

This is a short stop to look at the undeformed granites. This stop is located where a narrow intrusion of Sixmile Granite along the Packsaddle/Valley Spring contact is adjacent to the Valley Spring gneisses (see Fig. 16). On the northwest side of the low water crossing, two generations of granite contain xenoliths of Valley Spring gneisses. One fine-grained granite is light pink in color and appears to be intruded by coarser grained, darker reddish granite. The later granite is found in dikes as well as in more amorphous shapes and appears to be less abundant than the fine-grained granite. Pegmatite veins cut across both granites and xenoliths and are the latest intrusive phase in this area.

Xenoliths of Valley Spring gneiss found within the granites at the low water crossing contain a well-developed S_2 foliation that is folded by F_3 folds. On the northeast side of the road outcrops of Valley Spring gneisses contain an isoclinally folded S_2 foliation. These outcrops do not appear to be xenoliths, suggesting there are only small granitic stringers exposed in this location.

Continue north on CR l03 for 2.3 miles, where it intersects Hwy 29. Turn right onto Hwy 29. At 10.2 miles Hwy 71 rejoins Hwy 29. Follow 29/71 to Llano. Follow Hwy 71 as it turns right and joins with Hwy 16. Continue on Hwy 71/16 for 0.1 miles.

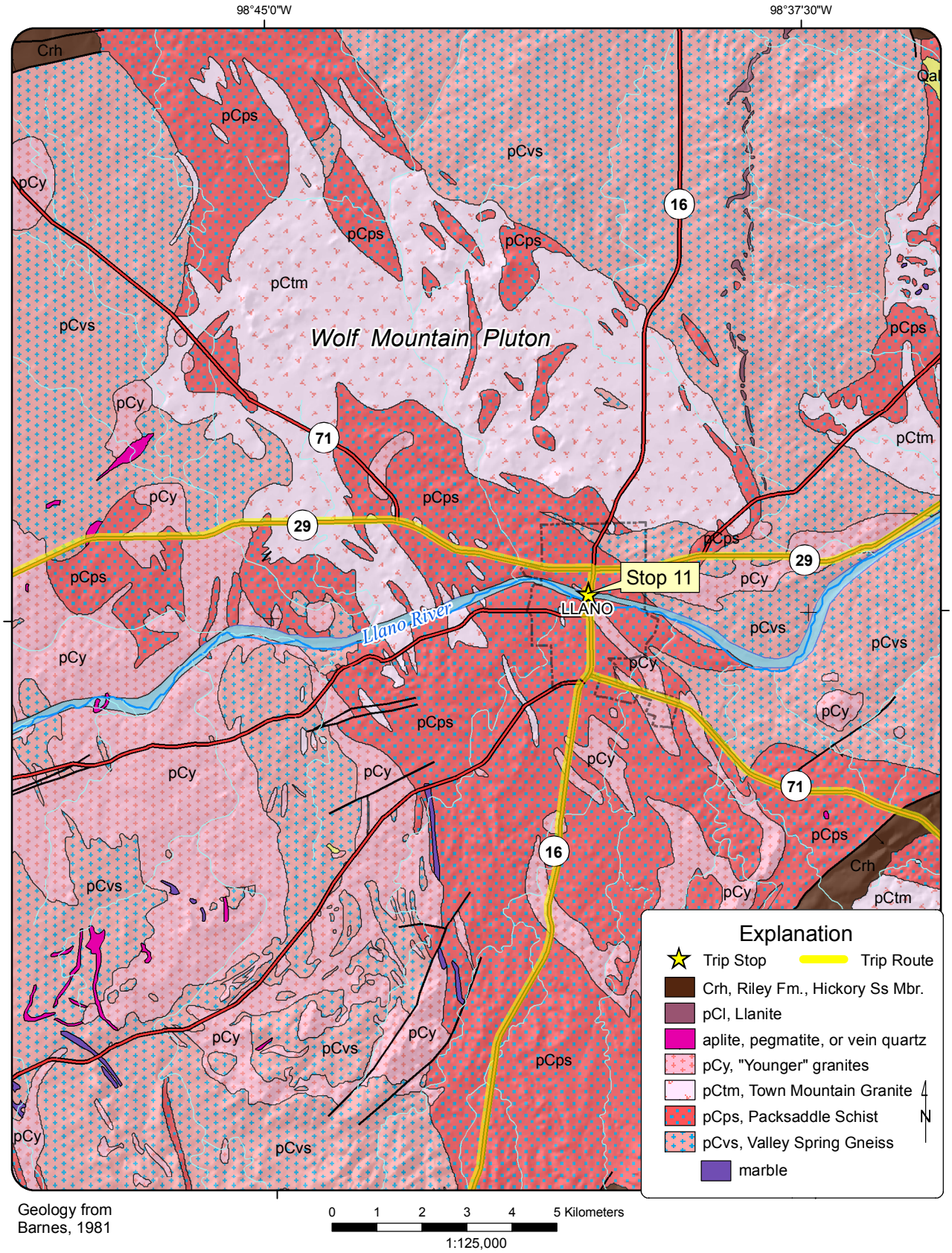

Figure 21. Geologic map of the region surrounding the city of Llano, showing the location of Stop 11.

Turn right onto W. Burnet St. immediately before the Llano River bridge. Pass the Llaneaux Restaurant and take the first left. Turn into a circle drive. Park here to look at rocks beneath the Llano bridge.

Stop 11. Folded and boudinaged granite sills and cross cutting dikes in Packsaddle domain, City of Llano, below the north bridge abutment of the Highway 16 bridge over the Llano River. *The following description is by M. A. Helper*

This outcrop, which is proximal to the 1118+/-5 Ma Wolf Mountain pluton and amidst smaller bodies of undated finer grained granite (Fig. 21), contains gray- and pink-banded gneisses of the Packsaddle domain that show a superbly developed mineral lineation on foliation surfaces that are folded by broad open folds. Gneiss and biotite schist here is intruded by two generations of granite that either cross-cut or are folded with the foliation. This outcrop permits observations of the relative sequence of plutonism, deformation, and dynamothermal and static metamorphism that define the last phases of the Precambrian history.

Lithologies:

1) Medium-grained gray-, black- and pale pink-banded hornblende-biotite-quartz-plagioclase-gneiss. Gneissic banding is defined by mafic- and felsic mineral-rich layers. In biotite-rich layers, a biotite ± hornblende foliation is parallel to banding. In felsic-rich layers, the gneissic layering contains an elongation lineation defined by elongate quartz and feldspar, and by linear concentrations of biotite and hornblende (Fig. 22). Unaligned hornblende and biotite record partial to complete static recrystallization of fabric forming minerals, as does late growing epidote and minor chlorite.
2) Biotite schist overlies and is interlayered with the gneiss. Contacts with gneiss are gradational, and schist layers (decimeter to meter thickness) increase in abundance upward. Schists are hornblende poor and biotite rich in comparison to gneiss, but are otherwise compositionally similar. Schistosity is defined by aligned biotite.
3) Biotite granite as sills within schist and gneiss. Medium- to coarse-grained pink microcline, gray quartz, white plagioclase and biotite give these a characteristic appearance. Boudinaged and folded sills of this granite, all less than a meter thick, are concordant to the foliation in schist and gneiss (Fig. 23). Igneous textures and mineralogy are well preserved; internal deformational fabric is not obvious in outcrop. Though not dated at this outcrop, the relative age and medium- to coarse-grained texture of these sills mostly closely resembles granite of the 1118 Ma Wolf Mountain pluton immediately to the north. As folded granite, they likely fall in the age range of 1126-1118 Ma.
4) Pegmatitic to aplitic granite dikes and veins, often with associated milky quartz veins and pods. Light to dark pink, up to ~1.5 m thick, with both straight and irregular margins; these cut all other lithologies and are unaffected by folding. The dike here have not been dated, but being little deformed were likely intruded in the interval 1116-1070 Ma.

Structure and intrusive relationships:

1) Gneissic layering (S0) the biotite±hornblende foliation/schistosity (S1-2) and biotite granite sills are folded by upright, open to closed, southeast-trending folds (F5) (Fig. 24). Closed folds are asymmetric with a westward vergence. Folds of the granite sills are coaxial to sub-parallel with the elongation lineation (L2) in the gneiss.
2) Boudinage of granite sills records extension parallel to the axis of F5 folding (Fig. 24). Boudin necks are filled by vein quartz that defines orientations that are conjugate with respect to F5 fold axes.
3) Pegmatitic to aplitic dikes cut folded and boudinaged granite sills and are themselves weakly boudinaged, recording extension in a SE-NW direction.

Figure 22. Mineral lineations in gray, quartz-feldspar-amphibole gneiss.

Figure 23. Boudinaged granite sill within biotite-hornblende schist.

Figure 24. Folded granite sill within hornblende-biotite-gneiss and biotite schist.

Retrace path to HW 16/71 and turn right (south). Just south of Llano, take HW 71 when it turns left (east) towards Austin. Drive 23.4 miles and turn left on CR 2147 into Horseshoe Bay. Drive 3.2 miles and turn left at sign for Ferguson Power Plant. Drive 1.8 miles to road cuts along both sides of the road. This is a short stop to look at the late-stage coarse grained granites.

Stop 12: Marble Falls (or Granite Mountain) Pluton; Coarse-grained Granite
The description below is modified from Barker et al. (1996; in Mosher, 1996).

Coarse-grained granitic plutons (Town Mountain Granite; the red unit on the map on the cover of this guidebook) in the Llano uplift make up 30% of the exposed area of Precambrian rock (Johnson and others, 1976). Most Llano granitic plutons in plan view are roughly circular, with diameters of 15 to 25 km. Gravity and magnetic surveys (summarized by Muehlberger et al., 1963) show that the intrusive contacts must be approximately vertical in at least the upper 2 or 3 km of preserved crust. Reed (1999) distinguishes two populations of coarse granite bodies in the Llano uplift. One forms elongated or irregular plutons showing solid-state deformation. The other group forms plutons that are ovoid or circular in plan with smoothly curving perimeters, subtle internal zonation that is generally parallel to the contact with wallrock, and weak foliation that apparently represents flow while above the solidus. The Marble Falls pluton is an example of the second group and has been dated at 1091 +/-2 (J. Connelly, unpubl. data).

The granite contains pink-rose K-feldspar megacrysts up to 4 cm long, gray-green to white plagioclase up to 2 cm, dark gray quartz in clusters up to 2.5 cm in diameter, and black biotite + amphibole in clots up to 1 cm diameter. K-feldspar commonly forms overgrowths on plagioclase, and more rarely plagioclase mantles K-feldspar, yielding the classic "rapakivi" texture (Wark and Stimac, 1992; Ramo and Haapala, 1995). Fine equigranular granitic ovoid inclusions, reaching 5 cm in diameter, are also mantled by K-feldspar. Plagioclase shows weak zoning; zircon and allanite show strong oscillatory zoning in backscattered electron images. Titanite is nearly colorless and anhedral, commonly enclosed by amphibole and biotite. Other accessory minerals are ilmenite, magnetite, apatite, fluorite, and pyrite. Chlorite, replacing biotite, and calcite and sericite, replacing plagioclase, are the only obviously secondary minerals.

Overall, plagioclase is $An_{4\text{-}22}Ab_{76\text{-}95}Or_{0.5\text{-}6}$, and K-feldspar is microcline, $An_{0\text{-}0.3}Ab_{2.2\text{-}10.7}Or_{89.3\text{-}97.5}$. The microcline is commonly microperthitic, containing albite lamellae with $An_{6.5}Ab_{91.3}Or_{2.2}$ as a representative composition. Myrmekite (an intergrowth, on a microscopic scale, of quartz and plagioclase) is uncommon, occurring at the boundaries between microcline and plagioclase. The strong rose-pink color of the K-feldspar is probably caused by fine disseminated hematite.

These granites have a juvenile Nd signature and geochemistry compatible with combined crustal and depleted mantle sources (Smith et al., 1997). Valley Spring gneiss could not have been the source of magma feeding the plutons; the gneiss has an initial $^{87}Sr/^{86}Sr$ ratio of 0.7128 ± 0.0007, but the Enchanted Rock and Lone Grove plutons have initial ratios, based on 9- and 13-point isochrons, respectively, of 0.7048 ± 0.0007

and 0.7061 ± 0.0003 (Garrison and others, 1979). The disparity in initial Sr isotopic ratios indicates that granite magmas, represented by these two plutons, could not have been generated by partial fusion of Valley Spring Gneiss. Instead, the Sr isotopic data indicate that the granites must have been derived, in large part, from upper mantle and/or lower crustal sources. Patchett and Ruiz (1989) give Sm-Nd data for some Llano granites, including a sample from the Granite Mountain quarry in the Marble Falls pluton; eNd for this sample is +3.4 at 1.06 Ga and, overall, the coarse pink Llano granites that were analyzed have eNd(t) from +2.6 to +3.8. These Nd data agree with the Sr isotopic compositions in indicating a significant mantle component in the granites.

To return to Austin, retrace the route back to Hwy 71 and turn left (east). Drive about 40 miles to Austin.

REFERENCES

Barnes, V. E., 1945, Soapstone and serpentine in the Central Mineral Region of Texas: Univ. Texas Pub. 4301, p. 55-91.

Barnes, V. E., 1978, Geologic Quadrangle Map No. 43: Geology of the Click Quadrangle, Llano and Blanco Counties, Texas: University of Texas Bureau of Economic Geology, scale 1:24,000.

Barnes, V. E., 1981, Geologic atlas of Texas - Llano sheet: University of Texas Bureau of Economic Geology, scale 1:250,000.

Bebout, G. E., and Carlson, W. D., 1986, Fluid evolution and transport during metamorphism: Evidence from the Llano Uplift, Texas: Contributions to Mineralogy and Petrology, v. 92, p. 518-529.

Carlson, W. D., 1998, Petrologic constraints on the tectonic evolution of the Llano uplift. *in* J.P. Hogan and M.C. Gilbert, eds., Basement Tectonics 12: Proceedings of the 12th International Conference on Basement Tectonics. Kluwer Academic Press, Dordrecht, p. 3-28.

Carlson, W. D., and Nelis, M. K., 1986, An occurrence of staurolite in the Llano Uplift, central Texas: American Mineralogist, v. 71, p. 682-685.

Carlson, W. D., and Johnson, C. D., 1991, Coronal reaction textures in garnet amphibolites of the Llano Uplift: American Mineralogist, v. 76, p. 756-772.

Carlson, W. D., and Schwarze, E. T., 1993, Petrologic and tectonic significance of geographic variations in garnet growth zoning in the Llano Uplift: Geological Society of America Abstracts with Programs, v. 25, no. 7, p. A101-102.

Carlson, W. D., and Reese, J. F., 1993, Petrologic significance of staurolites in the Llano Uplift: Geological Society of America Abstracts with Programs, v. 25, no. 1, p. A5.

Carlson, W. D., and Reese, J. F., 1994, Nearly pure iron staurolite in the southeastern Llano Uplift, Texas and its petrologic significance: American Mineralogist, v. 79, p. 154-160.

Carlson, W.D., Anderson, S.D., Mosher, S., Davidow, J.S., Crawford, W.D., and Lane, E.D., 2007, High-pressure metamorphism in the Texas Grenville orogen: Mesoproterozoic subduction of the southern Laurentian continental margin: International Geology Review, v. 49, p. 99–119.

Carter, K. E., 1989, Grenville orogenic affinities in the Red Mountain area, Llano Uplift, Texas: Canadian Journal of Earth Sciences, v. 26, p. 1124-1135.

Carter, K. E., Reese, J., and Helper, M. A., 1993, Precambrian extension in the Llano Uplift: Geological Society of America Abstracts with Programs, v. 25, no. 1, p. A5.

Flawn, P. T., and Muehlberger, W. R., 1970, The Precambrian of the United States of America; South-Central United States, *in* Rankama, K. (ed.), The Geologic Systems, The Precambrian: Interscience, v. 4, p. 72-143.

Garrison, J. R., Jr., 1979, Petrology and geochemistry of the Precambrian Coal Creek Serpentinite mass and associated metamorphosed basaltic and intermediate rocks, Llano Uplift, Texas [Ph.D. dissertation]: Austin, Texas, University of Texas, 262 p.

Garrison, J. R., Jr., 1981a, Coal Creek Serpentinite, Llano Uplift: A fragment of a Precambrian ophiolite: Geology, v. 9, p. 225-230.

Garrison, J. R., Jr., 1981b, Metabasalts and metagabbros from the Llano Uplift, Texas: Petrologic and geochemical characterization with emphasis on tectonic setting: Contributions to Mineralogy and Petrology, v. 78, p. 459-475.

Garrison, J.R., Jr., 1982, Metabasalts and metagabbros from the Llano Uplift, Texas: petrologic and geochemical characterization with emphasis on tectonic setting: Contributions to Mineralogy and Petrology, v. 78, p. 459–475, doi: 10.1007/BF00375208.

Garrison, J. R., Jr., 1985, Petrology, geochemistry, and origin of the Big Branch and Red Mountain Gneisses, southeastern Llano Uplift, central Texas: American Mineralogist, v. 70, p. 1151-1163.

Garrison, J. R., Jr., Long, L. E., and Richmann, D. L., 1979, Rb-Sr and K-Ar geochronologic and isotopic studies, Llano Uplift, central Texas: Contributions to Mineralogy and Petrology, v. 69, p. 361-374.

Gillis, G., 1989, Polyphase deformation of the Middle Proterozoic Coal Creek Serpentinite, Llano Uplift, Texas [M.A. thesis]: Austin, Texas, University of Texas, 88 p.

Gillis, G., and Mosher, S., 1988, Polyphase deformation of the Middle Proterozoic Coal Creek Serpentinite: Geological Society of America Abstracts with Programs, v. 20, no. 2, p. A99.

Gobel, V. W., 1992, Middle Proterozoic eclogitogenic metabasites in Llano County, central Llano Uplift, Texas: Geological Society of America Abstracts with Programs, v. 24, no. 1, p. A?.

Graham, C. M., and Powell, R., 1984, A garnet-hornblende thermometer and application to the Pelona Schist, southern California: Journal of Metamorphic Geology, v. 2, p. 13–32.

Hoh, A. M. 2000, Deformational history of the Valley Spring Domain in the northeastern Llano Uplift, Devil's Waterhole, Inks Lake State Park, Burnet County, Texas. [unpublished M.A. the sis], The University of Texas at Austin, 139p.

Hoh, A., 2004, Structural history of the Valley Spring domain exposed in Devil's Waterhole, Inks Lake State Park, Burnet County, Texas,: *in* Hoh, A., and Hunt, B., eds., Tectonic History of southern Laurentia: A look at Mesoproterozoic, Late-Paleozoic, and Cenozoic Structures in Central Texas, Austin Geological Society Field Trip Guidebook 24.

Hunt, B.B., 2000, Mesoproterozoic structural evolution and lithologic investigation of the western Llano uplift, Mason County, Texas. MS thesis, University of Texas at Austin, 139 p.

Hunt, B., Helper, M. and Roback, R., 1996, Structural relations among Precambrian granite, gneiss and amphibolite in an outcrop of Packsaddle Schist, western Llano Uplift, central Texas. Geological Society of America Abstracts with Programs, 30th South-Central Section Meeting, v.28, no. 1, p. 20. .

Johnson, L. A., Rogers, J. J. W., and Nagy, R. M., 1976, Composition of the Precambrian Llano Uplift, central Texas, U.S.A. Geochimica et Cosmochimica Acta 40: 1419-1420.

Letargo, C. M. R., Lamb, W. M., and Park, J.-S., 1995, Comparison of calcite + dolomite thermometry and carbonate + silicate equilibria: Constraints on the conditions of metamorphism of the llano uplift, central Texas, U. S. A. American Mineralogist 80: 131-143.

Levine, J., 2005, Structural analysis and detrital zircon provenance in the western Llano Uplift: Implications for a southern collider [Unpublished M.S. thesis]: The University of Texas at Austin, p. 140.

Levine, J., Hunt, B. and Mosher, S., 2004, Grenville-Age Tectonic Evolution, Western Llano Uplift, Central Texas: *in* Transactions from Gulf Coast Association of Geological Societies 54th Annual Convention, San Antonio, Texas, October 10-12, 2004.

Johnson, L. A., Rogers, J. J. W., and Nagy, R. M., 1976, Composition of the Precambrian Llano Uplift, central Texas, U.S.A. Geochimica et Cosmochimica Acta 40: 1419-1420.

McGehee, R. V., 1979, Precambrian rocks of the southeastern Llano region, Texas: University of Texas Bureau of Economic Geology Circular 79-3, 36 p.

Mosher, S., 1993, Exposed Proterozoic rocks of Texas (part of "Proterozoic rocks east and southeast of the Grenville Front"), *in* Reed, J. C. and many others, eds., Precambrian: Conterminous U.S.: Boulder, Colorado, Geological Society of America, The Geology of North America, v. C-2, p. 366-378.

Mosher, S., 1996, Guide to the Precambrian Geology of the Eastern Llano Uplift: editor and major contributing author, South-Central Geological Society of America Meeting, Austin, TX, March, 1996, 78p.

Mosher, S., 1998, Tectonic evolution of the southern Laurentian Grenville orogenic belt: Geological Society of America Bulletin, v. 110, no. 11, p. 1357–1375, doi: 10.1130/0016-7606(1998)110<1357:TEOTSL>2.3.CO;2.

Mosher, S., 2004, Tectonic History of the Llano Uplift: *in* Hoh, A., and Hunt, B., eds., Tectonic History of southern Laurentia: A look at Mesoproterozoic, Late-Paleozoic, and Cenozoic Structures in Central Texas, Austin Geological Society Field Trip Guidebook 24.

Mosher, S., Hoh, A.M., Zumbro, J.A., and Reese, J.F., 2004, Tectonic Evolution of the Eastern Llano Uplift, central Texas: A record of Grenville orogenesis along the southern Laurentian margin, in Tollo, R.P., Corriveau, L., McLelland, J., and Bartholomew, M. J., eds., Proterozoic Tectonic Evolution of the Grenville Orogen in North America: Geological Society of America Memoir 197, p. 783–798.

Mosher, S., Levine, J.S.F, and Carlson, W.D, 2008, Mesoproterozoic plate tectonics: A collisional model for the Grenville-aged orogenic belt in the Llano uplift, central Texas. Geology, v. 36, p. 55-58; DOI 10.1130/G24049A.1.

Muehlberger, W. R., Bhatrakarn, T., and Youash, Y. Y., 1963, Correlation of geology and gravity observations in southern Burnet County, Texas. Texas Journal of Science 15: 35-49.

Muehlberger, W. R., Denison, R. E., and Lidiak, E. G., 1967, Basement rocks in the continental interior of the United States: American Association of Petroleum Geologists Bulletin, v. 12, p. 2351-2380.

Nelis, M. K., Mosher, S., and Carlson, W. D., 1989, Grenville-age orogeny in the Llano Uplift of central Texas: Deformation and metamorphism of the Rough Ridge Formation: Geological Society of America Bulletin, v. 101, p. 876-883.

Patchett, P. J., and Ruiz, J., 1989, Nd isotopes and the origin of Grenville-age rocks in Texas: Implications for Proterozoic evolution of the United States mid-continent region: Journal of Geology, v. 97, p. 685-695.

Ramo, O. T., and Haapala, I., 1995, One hundred years of Rapakivi Granite. Mineralogy and Petrology 52: 129-185.

Reed, R.M., 1999. Emplacement and deformation of late syn-orogenic to post-orogenic Mesoproterozoic granites in the Llano Uplift, central Texas [unpublished Ph.D. dissertation]: University of Texas at Austin.

Reed, R. M., Roback, R. C., and Helper, M. A., 1995, Nature and age of ductile deformation associated with the "anorogenic" Town Mountain Granite, Llano Uplift, central Texas. 12th International Conference on Basement Tectonics, in press

Reed, R.M., Eustice, R.A., Rougvie, J.R., Reese, J.F., 1996, Sedimentary structures, paleo-weathering, and protoliths of metamorphic rocks, Grenvillian Llano Uplift, Central Texas: Geological Society of America Abstracts with Programs, v. 28, no. 1, p. 59.

Reese, J. F., 1995, Structural evolution and geochronology of the southeastern Llano Uplift, central Texas. [Ph.D. dissertation]: Austin, Texas, University of Texas, 172 p.

Reese, J.S., Mosher, S., Connelly, J., and Roback, R., 2000, Mesoproterozoic chronostratigraphy of the southeastern Llano Uplift, central Texas: Geological Society of America Bulletin, v. 112, no. 2, p. 278–291, doi: 10.1130/0016-7606(2000)112<0278:MCOTSL>2.3.CO;2.

Reese, J.S., and Mosher, S., 2004, Kinematic constraints on Rodinia reconstructions from the core of the Texas Grenville Orogen: The Journal of Geology, v. 112, p. 185–205, doi: 10.1086/381657.

Roback, R.C., 1996, Characterization and tectonic evolution of a Mesoproterozoic island arc in the southern Grenville Orogen, Llano uplift, central Texas: Tectonophysics, v. 265, p. 29–52, doi: 10.1016/S0040-1951(96)00145-X.Smith, D.R., Barnes, C., Shannon, W., Roback, R., and James, E., 1997, Petrogenesis of mid-Proterozoic granitic magmas: examples from central and west Texas: Precambrian Research, v. 85, p. 53–79, doi: 10.1016/S0301-9268(97)00032-6.

Roback, R., Mosher, S., and Carlson, W. D., 1994, Evolution of the ~1.3 Ga Coal Creek island-arc terrane, Llano Uplift, central Texas: Geological Society of America Abstracts with Programs, v. 26, no. 7, p. A405.

Roback, R., James, E. W., and Whitefield, C. and Connelly, J., 1995 Tectonic assembly of "Grenville" terranes in the Llano Uplift, central Texas: Evidence from Pb and Sm-Nd isotopes: Geological Society of America Abstracts with Programs, v. 27, no. 6, p. A398

Roback, R.C., Hunt, B.B., and Helper, M.A., 1999, Mesoproterozoic tectonic evolution of the western Llano uplift, central Texas: The story in an outcrop: Rocky Mountain Geology, v. 43, p. 275-287.

Rougvie, J.R., Carlson, W.D., Copeland, P., and Connelly, J.N., 1999, Late thermal evolution of Proterozoic rocks in the northeastern Llano Uplift, central Texas: Precambrian Research, v. 94, pp. 49-72.

Smith, D. R., Barnes, C., Shannon, W., Roback, R., James, E., 1997, Petrogenesis of mid-Proterozoic granitic magmas: examples from central and west Texas: Precambrian Research, v. 85, p. 53-79.

Walker, N. W., 1992, Middle Proterozoic geologic evolution of the Llano Uplift, Texas: Evidence from U-Pb zircon geochronometry: Geological Society of America Bulletin, v. 104, p. 494-504.

Wark, D. A., and Stimac, J. A., 1992, Origin of mantled (rapakivi) feldspars: experimental evidence of a dissolution- and diffusion-controlled mechanism. Contributions to Mineralogy and Petrology 111: 345-361.

Whitefield, C. 1997. A Sm-Nd isotopic study of the Coal creek domain and Sandy Creek shear zone: [unpublished M. A. thesis], The University of Texas at Austin.

Wilkerson, A., Carlson, W. D., and Smith, D., 1988, High-pressure metamorphism during the Llano orogeny inferred from Proterozoic eclogitic remnants: Geology, v. 16, p. 391-394.

Zumbro, J., 1999, A structural, petrologic, and geochemical investigation of the Valley Spring Gneiss of the southeastern Llano Uplift, central Texas. [unpublished M. A. thesis], The University of Texas at Austin. 428 p.